공학박사학위논문

Optical properties in $MgAl_2O_4$ phosphor

$MgAl_2O_4$ 형광체의 광학적 특성에 관한 연구

2013년 2월

Department of Materials Science and Engineering
Seoul National University
임 재 혁

Optical properties in $MgAl_2O_4$ phosphor

$MgAl_2O_4$ spinel 형광체의 광학적 특성에 관한 연구

지도교수 **강 신 후**

이 논문을 공학박사 학위논문으로 제출함

2013년 2월

서울대학교 대학원

재료공학부

임 재 혁

임 재 혁의 공학박사 학위논문을 인준함

2013년 2월

위 원 장	홍 성 현	인
부위원장	강 신 후	인
위 원	남 기 태	인
위 원	김 창 해	인
위 원	김 용 선	인

Optical properties in $MgAl_2O_4$ phosphor

Advisor : Shinhoo Kang

by

Jaehyuk Lim

2013.02

Department of Materials Science and Engineering

Graduate School

Seoul National University

Abstract

$MgAl_2O_4$ spinel has been used for many applications because it has interesting electrical, mechanical, magnetic, and optical properties. Moreover, $MgAl_2O_4$ spinel is a well-known host material for luminescence. White emission produced by Ti-doped $MgAl_2O_4$ phosphor is reported, which is in contrast to blue emission from most Ti-doped single crystals of $MgAl_2O_4$. The emission characteristics are explained using energy diagrams obtained from a first-principle program, DV-Xα. The white emission peak consists of 4 deconvoluted peaks: 440, 490, 550, and 620 nm, when excited by 250 nm. Ti^{3+} in tetrahedral sites and Ti^{4+} in octahedral sites were found to contribute to greenish blue emissions at 490 and 550 nm. The red emission at 620–710 nm was produced by Mg^{2+} and O^{2-} vacancies.

Also Ti doped nano $MgAl_2O_4$ is synthesized by combustion method. Like in bulk system, the white emission is observed but containing blue color due to relatively large contents of Ti^{3+}. The emission spectrum at 250nm excitation can be separated to 4 peaks similar to bulk system. It indicates that the emission mechanism is caused by the same process at 250nm excitation.

On the other hand, Ti is occupied on the surface in nano $MgAl_2O_4$ as an emission source. As a result, the bluish white emission is obtained at 360nm excitation. Ti-doped $MgAl_2O_4$ is an interesting phosphor because it can provide white emission from a single host material without using rare earth elements.

Meanwhile, transmittance and green emission are obtained from sintered body of Ti doped $MgAl_2O_4$ by spark plasma sintering(SPS). After sintering, green emission is confirmed due to heat treatment in vacuum because Ti^{3+} mainly existed due to reduction atmosphere not the same as the white emission. Ti doped $MgAl_2O_4$ can attract attention due to tunable emission color such as green and white emission but more importantly fact that non rare earth is used.

Key word: $MgAl_2O_4$, phosphor, rare earth, nano, transparent, white emission

Student number: 2005-20947

Contents

List of Figures

1. Introduction

1.1 Current study on phosphor for W-LED

Phosphor materials have been researched for application as light source in display market. Many methods have been suggested for white LED through color blending. Primarily approach is to spread, red, green and blue phosphors on UV-LED. In the second approach is to use yellow phosphor on blue LED for white emission.[1-2] The later method is the most well known fabrication method for W-LED. Yellow phosphor, YAG:Ce is considered as one of the candidate due to its excitation at near 450nm in visible range which perfectly satisfies the condition.[3]

YAG:Ce yellow phosphor is widely used for outdoor fluorescent lamp but it shows relatively low CRI due to its low emission near red range. Hence, yellow phosphor like SiAlON:Eu^{2+} is used for indoor fluorescent lamp for this reason.[4] However, these kinds of phosphor have an inherent limitation of using the rare earth materials. In case of rare earth, it is possible to become strategic resource because 90% of its productivity is leaned on by China according to the column in “Independent” January 2010. Also the need of new phosphor draws attention from many researcher because Japan already took the advantageous position first with patents.[5] Aspect of this fact, recently, a rare earth-less phosphor by single host was successfully synthesized for white emission in our result.

Transition metal is considered for replacement of rare-earth in phosphor. Recently, a variety of materials such as Ti, V, Cr, Ni, Mn and Co on the same periodic lines

are regarded as doping like.[7-9] $MgAl_2O_4$ phosphor has been researched for host lattice with doped transition metal because $MgAl_2O_4$ is well known for an outstanding optical, mechanical property as well as chemical stability. In case of Cr doped Al_2O_3 and $MgAl_2O_4$, fabrication for laser materials has been studied as host materials because of its excellent luminescent property by additives. The solid state reaction is generally used for synthesis of powder and it seems to be at an advantage because of mass production.

Many researchers have been attempted to obtain nano sized phosphor due to strong emission intensity of Al_2O_3 and $MgAl_2O_4$.[4] Generally, nano sized phosphor shows a different luminescence property compare to bulk system because nano sized phosphor consists relatively higher numbers of defects. However, sometimes, the luminescence property can be decayed by several defects in nano sized phosphor. In spite of this disadvantage, the research, which is based on many kinds of characteristics about nano materials, has steadily attracted attention to many researchers. In this study, nano Ti doped $MgAl_2O_4$ was synthesized for comparison of luminescence property with bulk Ti doped $MgAl_2O_4$

Meanwhile, many cases about transition metal doped $MgAl_2O_4$ have been reported by single crystal growth.[7-9] In this case, both transmittance and luminescence properties can be obtained at the same time. It can be thought that the transmittance of single crystal $MgAl_2O_4$ is similar to that of poly-crystalline $MgAl_2O_4$ which is sintered by high temperature and high pressure. $MgAl_2O_4$ as transparent ceramics is researched for replacement of bullet-proof glass up to now

because of high transmittance and high mechanical property. In case of poly-crystalline $MgAl_2O_4$ without using single crystal growth, only transmittance was observed and luminescence property was not reported yet. Phosphor of thin film has also been studied as a thin film and if the phosphor with both transmittance and luminescence property can be synthesized easily, then it implies that the phosphor can be fabricated in industry field much more easily.

Our group has successfully obtained the sintered body of Ti doped $MgAl_2O_4$ which have both of these characteristics. Moreover, the synthesis method is more comfortable by high pressure and temperature compare to single crystal growth. Also it expects that the study of transparent $MgAl_2O_4$ will become more activated because recently, transparent $MgAl_2O_4$ has been synthesized by high temperature and pressure as well as in vacuum sintering without pressure.

Although the luminescent efficiency and emission as excitation by visible range must be improved in order to apply for a variety of display market, we expect that these problems can be overcome through additional research near in the future.

1.2 Objectives of the study

In this study, firstly, oxide was used for phosphor material as host lattice. $MgAl_2O_4$ was selected among oxide material as for its outstanding thermal, chemical stability and mechanical property. It expects that white emission can be accomplished using transition metal which is easily approached. Ti dopant was selected to synthesize, as for recent issue of fabricating white-LED with a strong emission property without using rare-earth, which Ti doping well reflects this aim.

Also, interpretation of emission mechanism is calculated using DV-Xα showing good reliability of density of state (DOS) and the energy band gap, which these calculations accord very well with experimental results.

Secondly, in order to understand the size effect on emission property, from bulk to nano, the difference of emission in part 2 were closely investigated. This nano powder was synthesized by combustion method. Activating emission through the defect level was considered in this part of investigation, using the fact that defects can be easily generated on the surface of nano material. Furthermore, the relationship between dopants and host was confirmed in microscopic view.

Lastly in part 4, bulk phosphors in part 2 were sintered at high temperature in a vacuum atmosphere in order to confirm the optical properties. Most of the previous research has been focused on just one characteristic between transmittance and luminescent property. Moreover, both of the characteristics were dealt with single crystal growth by some researchers which involve difficult tasks to overcome. In this study, both of the characteristics can be obtained in polycrystalline $MgAl_2O_4$

and these characteristics are analyzed from the relationship of Ti doping.

Part.2 A white emission phosphor about $MgAl_2O_4$ oxide system without rare-earth dopants

2.1 Introduction

White LED is getting more attentions as a new lighting source. It provides high energy efficiency with a long life and is environmentally friendly compared with conventional incandescent bulbs or fluorescent lamps. Development of appropriate phosphor materials, which can effectively convert electromagnetic waves generated from semiconductor to visible lights, is one of the most important technologies for efficient use of LEDs. White emission has been generally achieved by combining blue emission from LED and yellow emission from a phosphor that converts blue light into yellow. The combination of GaInN or GaN with YAG:Ce phosphor is currently the most successful example.

Recently, UV-LEDs have actively been investigated, which use a UV emitting chip as an excitation source to provide white light from mixtures of red, green, and blue phosphors. This design can improve the deficiency in color rendering of white emission, which is encountered by YAG:Ce phosphor along with blue LED[1,2]. The excitation wavelength of phosphors for UV-LEDs is required to have a large overlap with the emission wavelength for high efficiency. Thus, the phosphor materials for UV-LEDs should be designed to have a high absorption in the range of 350~410 nm, corresponding to the emission wavelength of UV-LEDs. Conventional

phosphors for CRT(cathode ray tube) and PDP(plasma display panel) cannot be used because they require significantly high energies for excitation.

$MgAl_2O_4$ spinel has been used for many applications because it has interesting electrical, mechanical, magnetic, and optical properties[3–6]. Moreover, $MgAl_2O_4$ spinel is a well-known host material for luminescence. Luminescence properties of $MgAl_2O_4$ doped with activators, such as Mn, Eu, V, Cr, or Ti have been reported[7–11]. In most cases the $MgAl_2O_4$-based luminescent materials are in the form of single crystal or prepared by sol–gel method. However, these synthetic methods are complicated and are found unsuitable for applications in lighting devices. White emission has been reported from a single host material with rare earth activator: nano MgO: Eu^{3+}.[12] The photoluminescence (PL) spectra showed a broad and weak emission in the range of 400–720 nm under excitation at 345 nm. In this system, hypersensitive transition ($^5D_0 \rightarrow {}^7F_2$) emission of Eu^{3+} was eminent among those from Eu^{3+} in MgO host. The $^5D_0 \rightarrow {}^7F_2$ transition is explained by non-inversion symmetry of nano MgO near the surface.

In this paper, we report white emission from Ti-doped $MgAl_2O_4$. As far as we know, a white-emitting phosphor of this kind, without the use of rare earth elements as activators, has never been reported[13-15].

2.2 Sample preparation

The samples were prepared from commercial $MgAl_2O_4$ (TSP-20, Taimei Chemicals Co. Ltd., Nagano, Japan) and TiO_2 (Nanotek, 99.95%, USA). TiO_2 powder was added to $MgAl_2O_4$ in the concentration range of 0.17~8.5 mol %. All powders were wet mixed homogeneously at 2000 rpm for 30 min in ethanol without using balls. The mixture of the powders was then fired at 1300 ℃ for 2 h in air and vacuum to produce Ti-doped $MgAl_2O_4$ (spinel). Next, the samples were ground to obtain powder for characterization.

2.3 Characterization methods

Photo-luminescent property was measured by a fluorescence spectrophotometer (Hitachi, F-4500, Japan). Excitation wavelength at 250 nm from a Xe lamp was used for PL measurement. The crystal structure was analyzed using X-ray powder diffraction (XRD, Rigaku D-max 2500, Japan). Distribution of Ti ions over the tetrahedral or octahedral sites or both in the spinel structure was calculated by Rietveld refinement of the XRD patterns (Topaz program). Oxidation states of Ti ions were analyzed using X-ray Photoelectron Spectroscopy (XPS, Sigma probe, ThermoVG, UK).

The energy diagrams of Ti-doped spinel were obtained using first-principle software, Discrete Variational Xα (DV-Xα) molecular orbital method, to interpret experimental results. With DV-Xα, various physical properties can be calculated through the integration of discrete variation. The molecular orbital result was explained by Mulliken method. The final values of electrical densities were calculated until the final result converges to initial value assumed before the numerical basis function was obtained[16]. This method approximates the exchange–correlation interaction with the Xα potential proposed by Slater and numerically solves the Schrödinger equation using the Hartree–Fock–Slater method. No restriction was imposed on the form of the basis functions because the calculation was conducted numerically[17,18]. There was no consideration in the calculation on the electron vibrations (modes), corresponding relaxation and nuclear transition in

the excited state. Even if this causes errors in absorption and emission wavelengths, still, this calculation method is believed to provide meaningful insights as to emission mechanisms based on band-to-band transition. The cluster model used for the calculation was $[Mg_{11}Al_{22}O_{55}]^{-22}$ in our study, which showed the convergence of the final values as mentioned above.

2.4 Results

The luminescence property is affected by the charge valence of dopants and the doping sites. The doping site was confirmed by Rietveld method and the charge valence was detected by XPS. The results of Rietveld analysis have detected Ti in both of sites. The content of Ti in tetrahedral site is 1.9 mol% and that of in octahedral site is 1.91 mol%. 1.7 mol% Ti doped spinel contains 1.9mol% TiO_2 in total, so the deviation between analysis and experimental data is small.

The occupied site of Ti was dealt with previous result. Also the charge valence of Ti was confirmed in fig. 2-1. In case of Ti doped $MgAl_2O_4$, Ti^{3+} and Ti^{4+} coexist in XPS results. The peak of Ti^{4+} was relatively high compare to that of Ti^{3+}. Generally Ti^{4+} is the most dominant phase among Ti ions and the XPS results by commercial TiO_2 and Ti_2O_3 also show the same tendency. The blue emission has been reported by Ti doped $MgAl_2O_4$. In this case, the sample was prepared by single crystal growth and the emission mechanism was explained by only Ti^{4+} in octahedral site. However, the result showed the coexistence of Ti^{3+} and Ti^{4+} through the XPS results and Ti is occupied in both of tetrahedral and octahedral site through Rietveld method about Ti doped $MgAl_2O_4$. This is in line with EXASF and NMR results of various spinels previously reported[20,21]. Based on the peak intensity in the figure, it was expected to have most Ti ions in the form of Ti^{4+}.

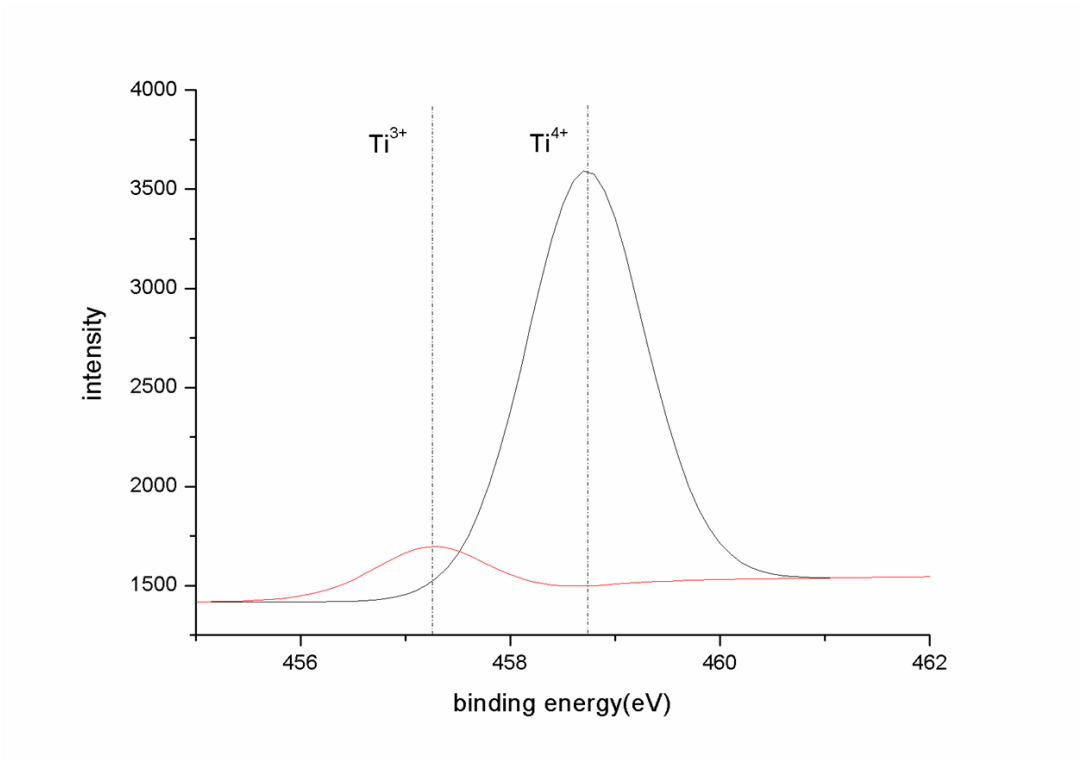

Fig.2-1 XPS results for the discrimination of Ti charge valence in Ti doped $MgAl_2O_4$

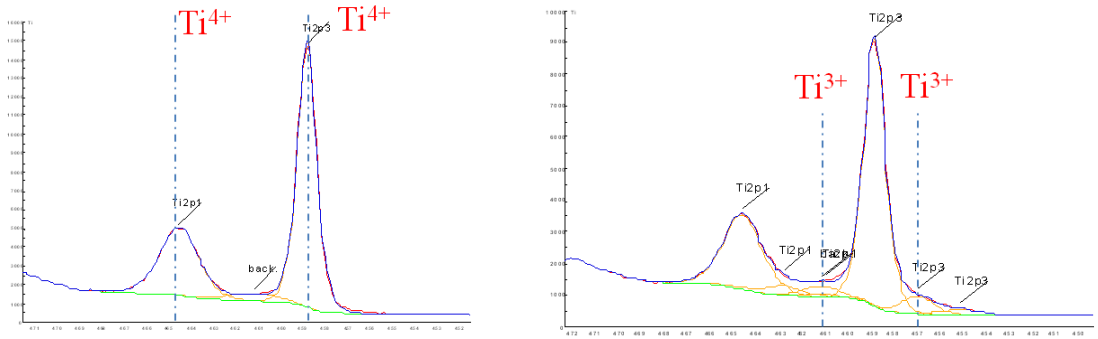

(a) Commercial TiO_2 (b) Commercial Ti_2O_3

Fig.2-2 XPS results for (a) commercial TiO_2, (b) commercial Ti_2O_3

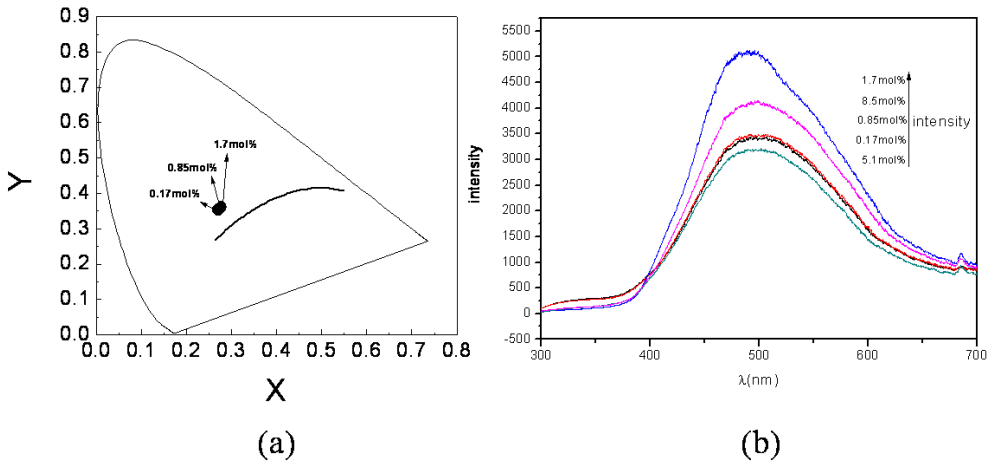

Fig.2-3 (a) chromaticity coordinate and (b) Concentration Quenching about Ti doped $MgAl_2O_4$

The chromaticity coordinates of Ti-doped $MgAl_2O_4$ powder are presented in 1931 CIE diagram, shown in Fig. 2-3a, as a function of Ti dopant concentration. According to the CIE diagram, the emission color is white with CIE coordinates (~0.35, ~0.28). This is similar to the coordinates of nano MgO: Eu^{3+}, (0.326~0.369, 0.263~0.322)[12]. Moreover, the concentration quenching of emission intensity was examined in the range of 0.17–8.5 mol % Ti dopant, the result is shown in Fig. 2-3b. As the Ti concentration increased, the emission intensity increased up to 1.7 mol % of Ti and then, it started decreasing. It was also found that with increasing of Ti contents, red shift occurred in CIE diagram within the range of 0.17–1.7 mol % Ti. It implies that the white color of this phosphor material could be tailored to certain extent.

XRD results of Ti doped $MgAl_2O_4$ are shown in fig.2-4. In order to confirm the solubility limit of Ti, powder is synthesized at 1500^{o}C-2h and doping contents are varied from 0% to 8.5mol%. The result shows that, TiO_2 segregation was not observed up to 8.5mol% Ti doping. Ti-doped single crystal $MgAl_2O_4$ is reported to have a broad emission at 490 nm. The 490 nm emission is explained by the presence of Ti^{4+} in the octahedral site of the spinel structure[9–11,22]. Although the 430 nm emission appeared at the peak shoulder, it was not discussed properly in the paper[9]. The emissions of 430 nm and 490 nm are also observed in Al_2O_3: Si, Ti owing to Ti^{4+} in octahedral site[23]. The 430 nm emission, however, was reasoned in the paper through the presence of carbon contamination. Fig. 2-5 shows the presence of 440

nm in the emission, which might be related to 430 nm emission of the previous work. Since we were not able to find carbon as an impurity in our system, it is most likely that Ti ions are responsible for both 440 and 490 nm emissions under 260 nm excitation. All these peaks were excited by 260nm wavelength after energy absorption as shown in Fig. 2-6.

We have looked at the emission mechanism through first-principle approach. We found that the calculation results match reasonably with the emissions shown in Fig. 2-5. In the calculations, we considered Ti^{3+} and Ti^{4+} in octahedral and tetrahedral sites and associated defects (vacancies). Fig. 2-8 shows the energy levels of Ti-doped spinel obtained from DV-Xα. In the figure, the dotted and solid lines stand for the energy levels unoccupied and occupied by electrons, respectively.

In addition, the electron contributions from Ti 3d and O2p orbitals are shown on the right side. The LUMO and HOMO levels, respectively the lowest unoccupied and the highest occupied molecular orbitals, of the Ti-doped $MgAl_2O_4$ are determined based on the energy diagram of undoped $MgAl_2O_4$ and the HOMO level was set at 0 eV for convenience.

The band gap energy of $MgAl_2O_4$ was calculated with the $[Mg_{11}Al_{22}O_{55}]^{-22}$ cluster as 9.15 eV using DV-Xα in fig.2-7, whereas the available experimental data are in the range of 7.5-9.0eV[24]. The cluster method with DV-Xα is known to predict band gap values larger than those from experiments due to quantum confinement effect of small cluster sizes. Our previous study by DV-Xa demonstrated that the band gap size of ZnO decreases to experimental values with increase of cluster size.[19]

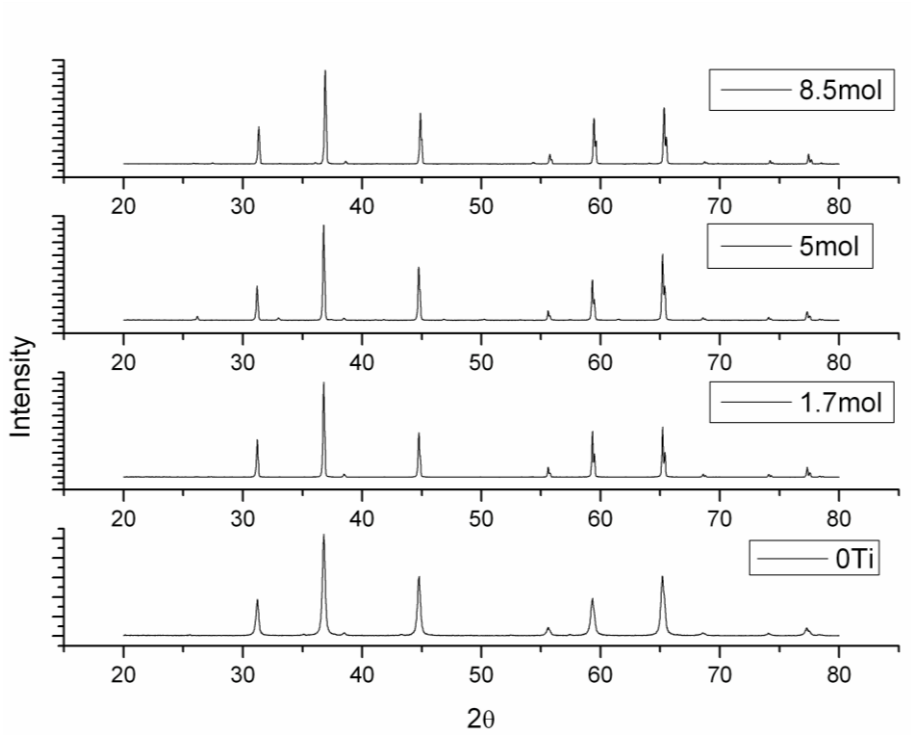

Fig.2-4 XRD results about x mol% Ti doped $MgAl_2O_4$ at 1500°C-2h(x=0, 1.7, 5, 8.5)

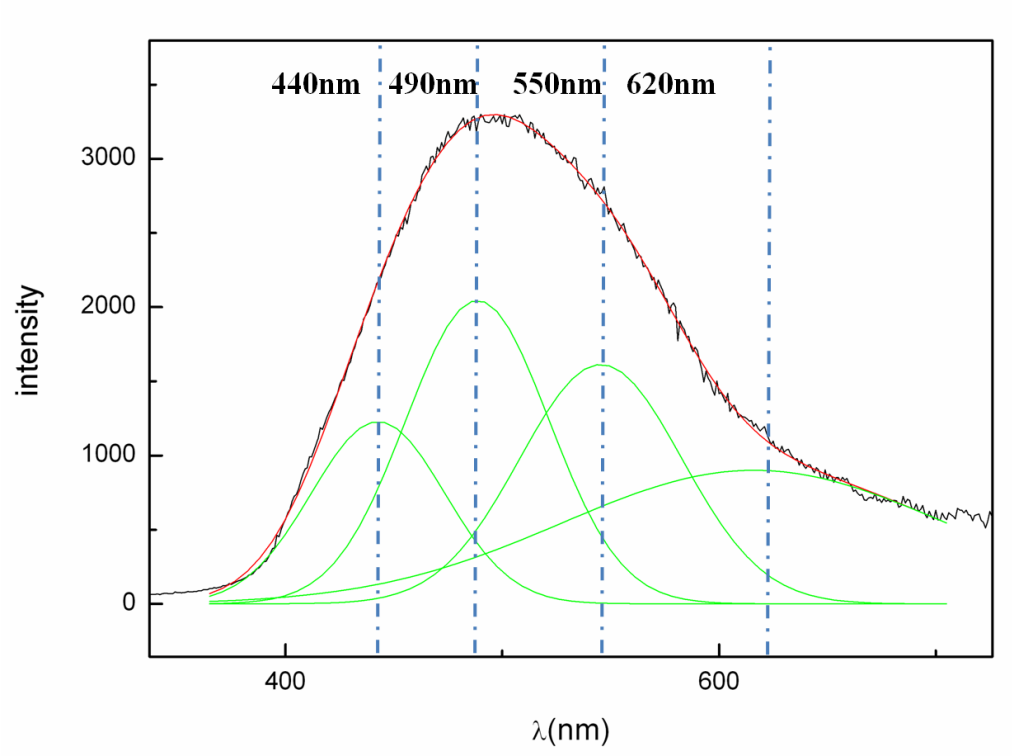

Fig.2-5 Deconvolution of Emission spectrum (Exc. 250nm)

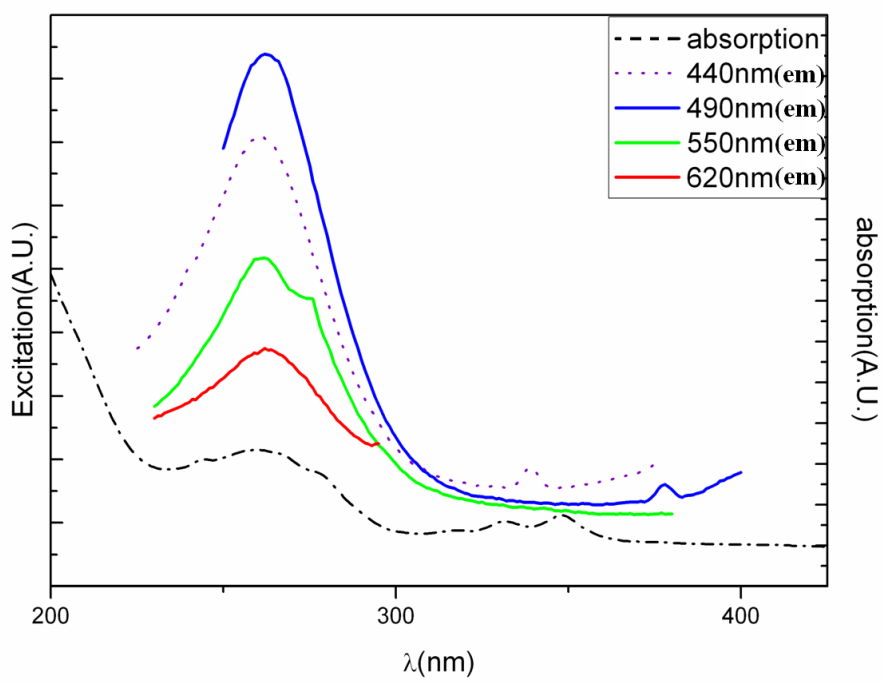

Fig. 2-6 Absorption and excitation spectra of 1.7 mole % Ti-doped $MgAl_2O_4$ phosphor

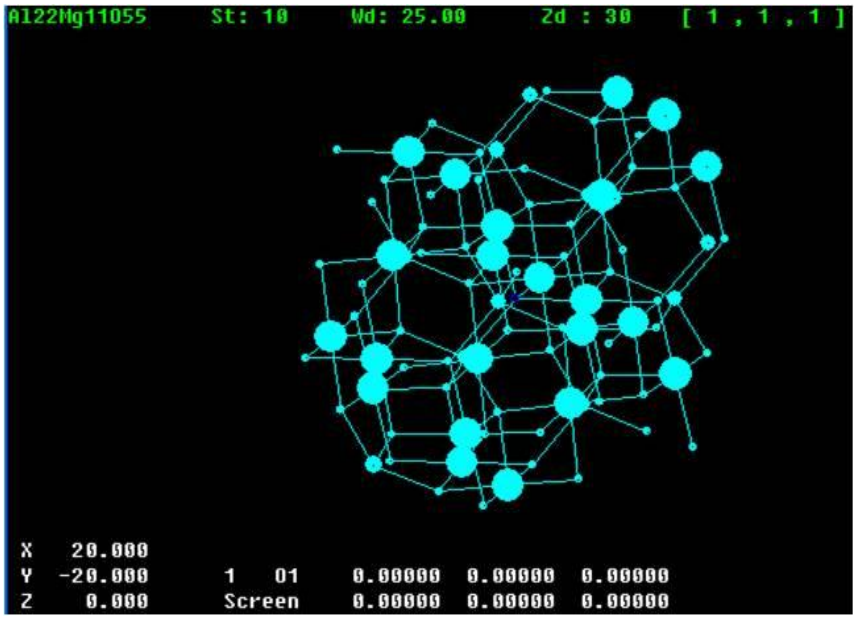

Fig. 2-7 $[Mg_{11}Al_{22}O_{55}]^{-22}$ cluster for calculation

The diameter of the $[Mg_{11}Al_{22}O_{55}]^{-22}$ cluster employed in this study is ~2.3nm and this might fall in the region of quantum confinement, causing larger separations between energy levels than those observed from bulk.

In Fig. 2-8, two energy levels were formed for Ti^{3+} ($3d^1$) in octahedral site, as usual[25]. Level 2 (^2E) associated with $3d_{z2}$ or $3d_{x^2-y^2}$ orbital was 5.6 eV higher than the HOMO level, while Level 1 ($^2T_2$), the ground state, which contains one electron in $3d_{xy}$, $3d_{yz}$, or $3d_{zx}$ orbital, was located 2.6 eV higher than the HOMO level. The energy gap, 3eV in the d orbital—ligand-field splitting parameter (Δ_{octa})— is due to the crystal field developed by oxygen ligands. In this case, the absorption of excitation wavelength from HOMO to ^2E is less likely due to low tendency of charge transfer in this case. However, a forced transfer from O2p by the absorption of 260nm excitation could occur, resulting in weak 413 and 480 nm emissions. During emission, the forbidden d–d transition from Level 2 to Level 1, $^2E \rightarrow {}^2T_2$, would be weakened further by the relaxation of parity selection rule. This broad transition with 413 nm (3 eV) and 480 nm emissions must be related to the 440 nm and 490 nm emission curves shown in Fig. 2-5, respectively. When Ti^{3+} ion occupies tetrahedral site, the electron located at $^2T_2$—the ground state—could be excited beyond LUMO level by the absorption of 260 nm excitation. Then, the electron transitions from LUMO to ^2E and to $^2T_2$ occur consequently, emitting 551 nm wavelength (2.25 eV).

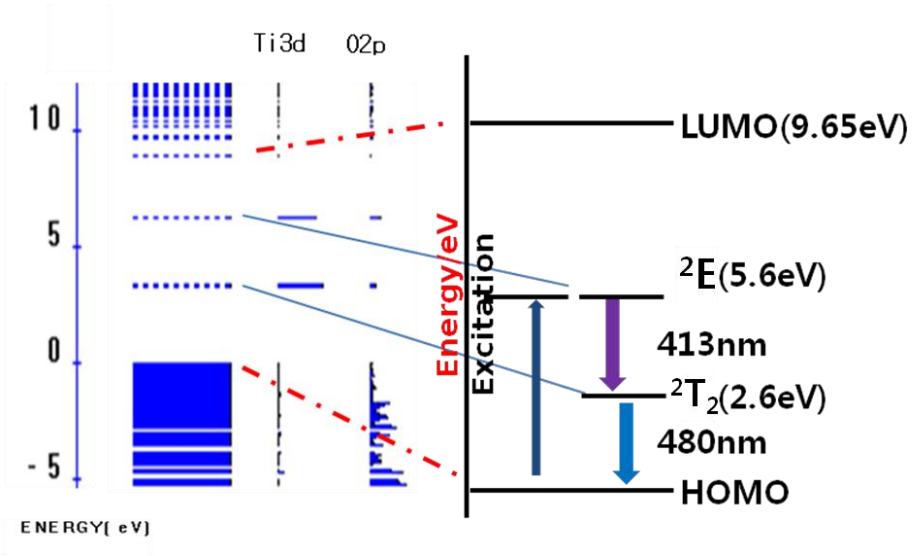

Fig.2-8 Ti^{3+} in octahedral site by calculation

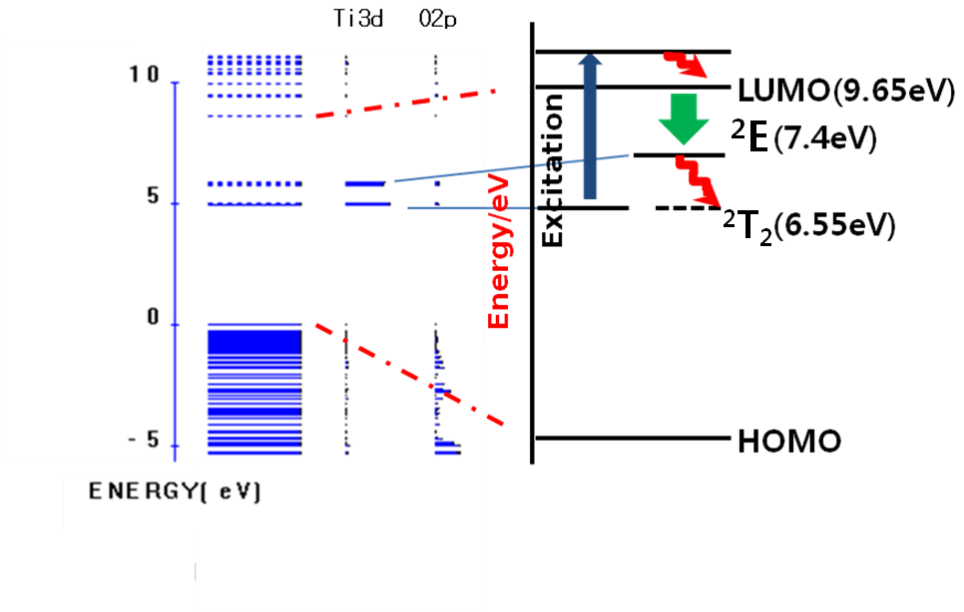

Fig.2-9 Ti^{3+} in tetrahedral site by calculation

Because this transition is allowed, a strong and broad emission is expected. The transitions between ^2E and $^2T_2$ and in the conduction band are nonradiative. The corresponding energy diagram is shown in Fig. 2-9.

Fig. 2-10 shows the energy diagram when Ti^{4+} ion ($3d^0$) occupies octahedral site. The calculation result shows that two energy levels are formed for the 3d orbitals, as in the case of Ti^{3+} in octahedral site. However, the energy gap between 3d orbitals, the difference between $^2T_2$ and ^2E, is smaller than that of Ti^{3+} in octahedral site, indicating weakened crystal field strength. Ti^{4+} has a tendency to be reduced, whereas Ti^{3+} tends to be oxidized. Thus, a charge transfer is much encouraged to Ti 3d (^2E) from O2p (HOMO), the energy difference of which is close to the excitation energy, ~ 5.0 eV. From the calculation we found that more than 95% of the HOMO level is occupied by the electrons of O2p orbital. When the charge transfer occurs, the empty ^2E of Ti^{4+} will obtain an electron, which will subsequently transit to $^2T_2$ and then, HOMO level, the ground state, result in 551 and 468 nm emissions (2.25 and 2.65 eV, respectively). Because this 468 nm emission is allowed, the peak intensity would be strong and broad, as shown in Fig. 2-5. However, the 551 nm (2.25 eV) emission is weak in this case because the transition is forbidden. This broad 468 nm emission matches reasonably with the results of Ti-doped single crystal spinel, a broad 490 nm emission in the previous study[9].

With Ti^{4+} in the tetrahedral site, the same charge transfer could occur between Ti 3d (Level 2) and O2p (HOMO), as in the case of Ti^{4+} in octahedral site shown in Fig. 2-10. However, the energy levels associated with 3d orbital are found much close to

the HOMO level, 1.9 and 2.5 eV for Level 1 and Level 2, respectively(fig.2-11). The ligand-field splitting parameter (Δ_{tet}) is 0.6 eV. Additionally, the energy levels were found almost continuous between HOMO and Level 1. Thus, all excited electrons, even if there are any by CT, return to the ground state nonradiatively by transition from Level 2 to Level 1, and subsequently to the ground state (HOMO). It is noted that emission from Ti^{4+} ion in the tetrahedral site is not expected at all.

When, however, Ti^{4+} takes tetrahedral site, as in the previous case, more Mg^{2+} vacancy would be formed for charge neutrality. A pure spinel was reported to have many intrinsic defects, such as Mg^{2+} and O^{2-} vacancies[9]. They often appear in pair, known as Schottky defects[26]. Fig. 2-12 shows the energy diagrams associated with Mg^{2+} and O^{2-} vacancies. Mg^{2+} vacancy generates Level 1 through Level 3 and thus, 620~710 nm (1.75~2 eV) emission becomes possible by transition from $^2T_2$ or Level 1 to the ground state (HOMO). On the other hand, in the case of O^{2-} vacancies, the calculated result shows that the excited electrons from the HOMO level to intermediate ^2E (5 eV) would transfer to Level 3 of Mg^{2+} vacancy (2.5 eV), emitting 496 nm peak wavelength. The electron transition between Level 3 and $^2T_2$ is nonradiative.

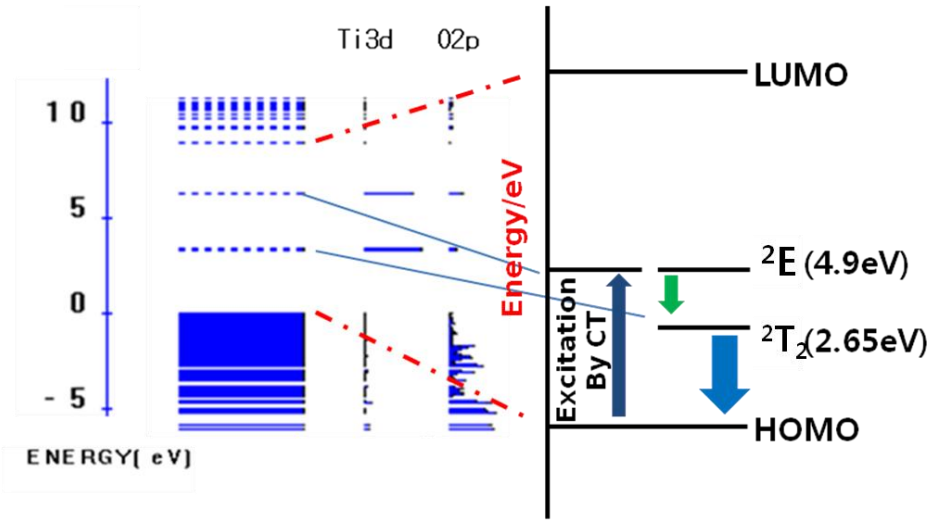

Fig.2-10 Ti^{4+} in octahedral site by calculation

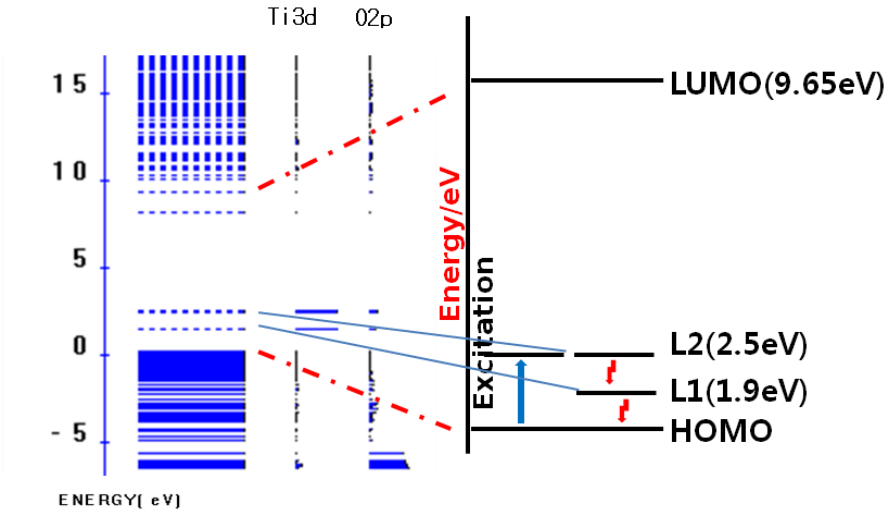

Fig. 2-11 Energy level for Ti^{4+} in tetrahedral site

It has been reported that 720 nm and 450 nm emissions from pure spinel are produced by Mg^{2+} vacancies[8–10]. Both peaks are reported to disappear when Mg becomes excessive in the system. Experimental result of this study indicates a strong transition from $^2T_2$ to the ground state (620 nm). The differences in the emission wavelengths exist between our experimental results with the previous results as to Mg^{2+} vacancies, which were 450, 720 nm vs. 490, 620 nm. It might imply that Level 1 and $^2T_2$ shift together to the ground state when the number of Mg^{2+} vacancies increases possibly by Ti^{4+} in tetrahedral site. It is to be noted that the energy diagrams in Fig. 2-12 represent the cases when Mg^{2+} and O^{2-} vacancies exist alone, not in pair. Nonetheless, the 490 nm (450 nm of previous report) emission should be attributed to the presence of the new energy level formed by O^{2-} vacancies.

The photoluminescence of the prepared phosphor showed a red shift, as shown in Fig. 2-13, when the synthetic temperature in air increased. It is because the formation of Mg^{2+} and O^{2-} vacancies is much facilitated at elevated temperatures, intensifying the 620 nm emission.

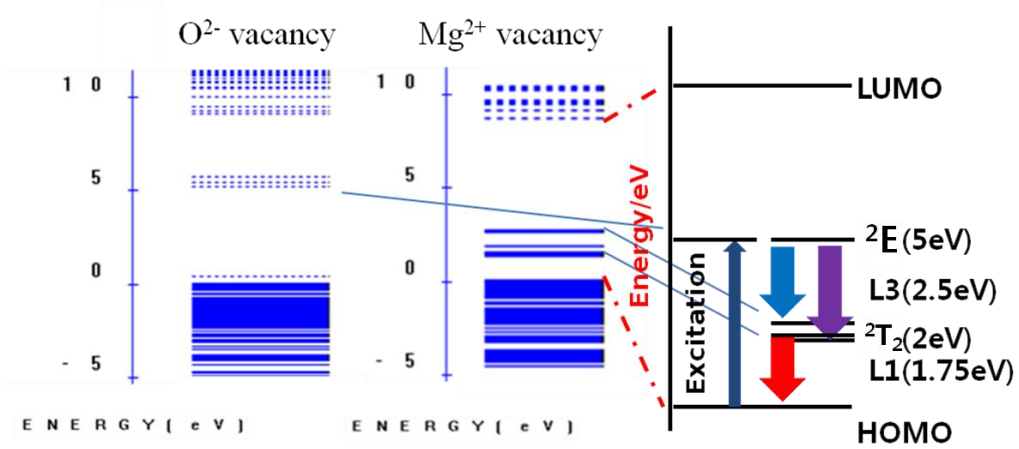

Fig.2-12 Schottky pair by Ti^{4+} in tetrahedral site

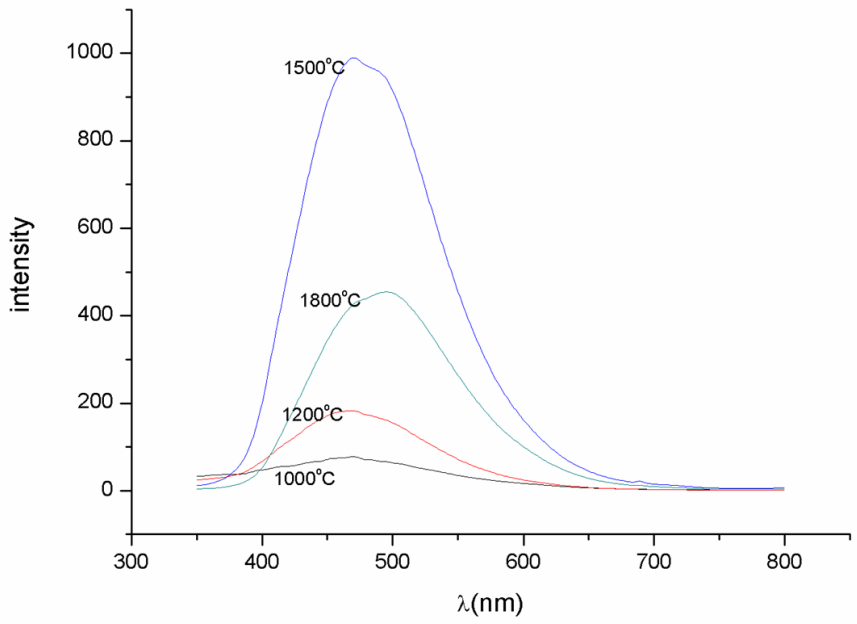

Fig.2-13 The PL results of Ti doped $MgAl_2O_4$ as the synthesized temperature

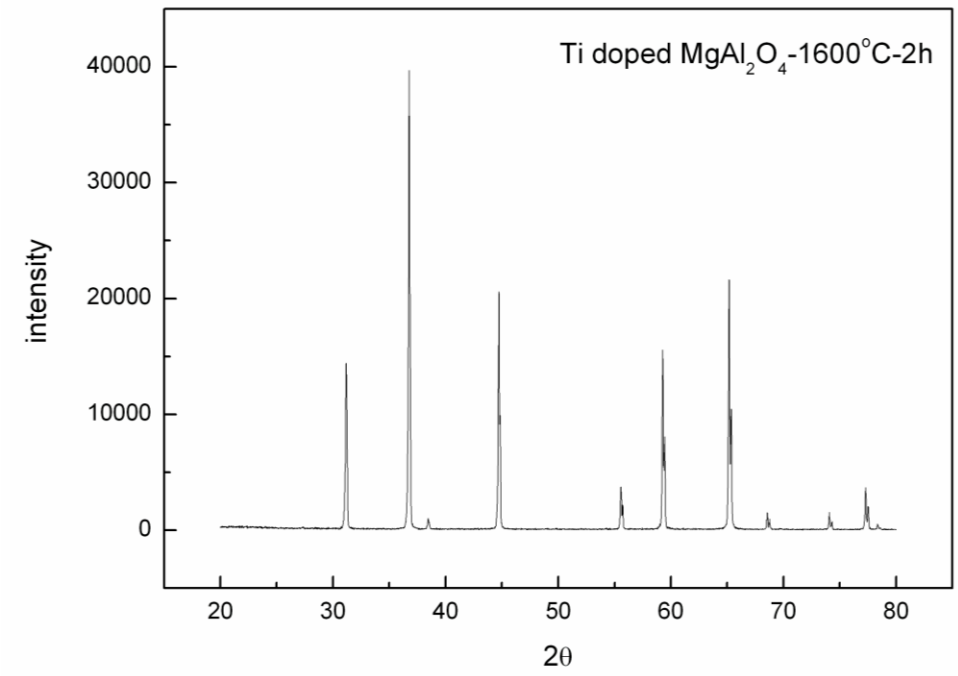

Fig.2-14 XRD result of Ti doped $MgAl_2O_4$ at 1600°C-2h

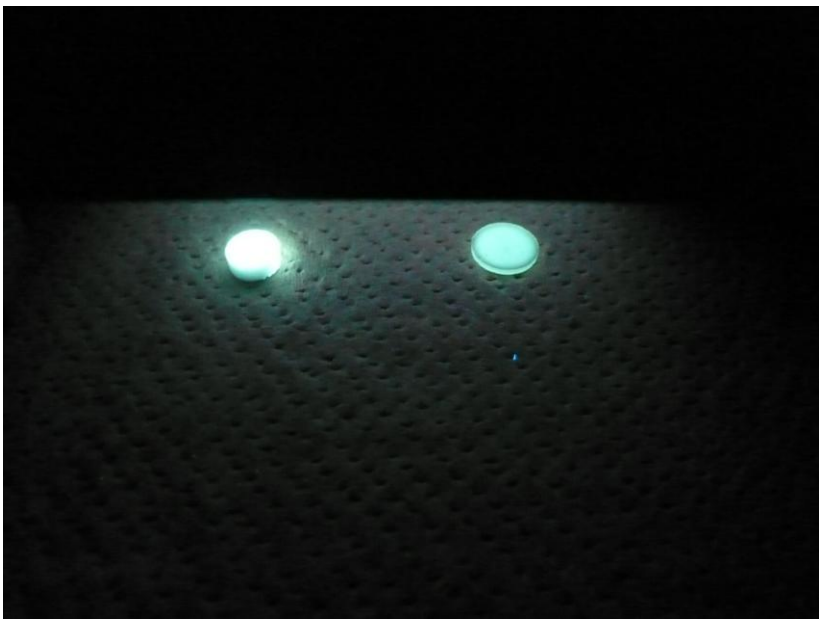

Fig.2-15 white(synthesis in air) and blue emission(synthesis in vac.) by heating condition

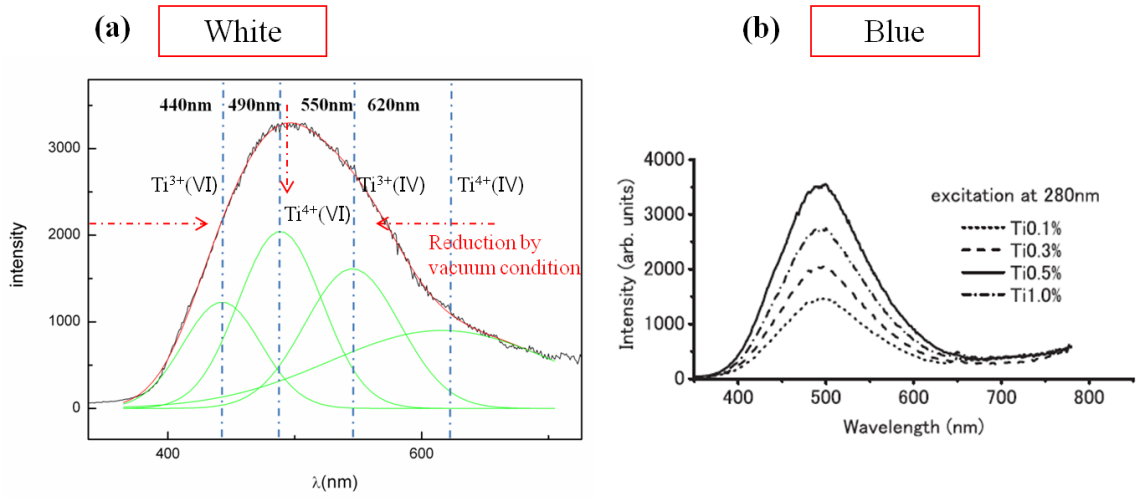

Fig.2-16 the difference of white(a: synthesis in air) and blue emission(b: synthesis in reduction condition) by heating condition

In case of synthesizing at higher temperature than 1500^{o}C, it predicts that the emission intensity is reduced because other phases can be segregated from Ti doped $MgAl_2O_4$. The XRD result of 1.7 mol% Ti doped $MgAl_2O_4$ at 1600^{o}C is shown in fig.2-14. According to XRD result, secondary phase cannot be detected. However, it has a possibility of segregation in Ti doped $MgAl_2O_4$, although the secondary phase cannot be observed due to low resolution of XRD. From fig.2-4, all phases are shifted to high angle as increasing Ti contents. On the other hand, the synthesis at high temperature like fig.2-14 is oppositely shifted to low angle. It predicts that Mg^{2+} or O^{2-} vacancies can be easily generated at high temperature and also these defects can be activated. It supports that oxygen vacancy is easy to be supplied aspect of thermodynamics in spite of oxidation condition. Therefore, it expects that PL intensity is decreased by these defects and secondary phases.

Furthermore, the chromaticity coordinate of white emission was found to change by the processing atmosphere. The Ti-doped spinel samples in Fig. 2-15 with white emission were synthesized in air and vacuum, respectively, using a super Kanthal furnace and spark plasma sintering. The emission color of those in air and vacuum changed from white to greenish blue. The vacuum condition intensified the 490 nm emission. If other factors remain unchanged, it implies that heat treatment in vacuum makes a relative increase of O^{2-} vacancies or relative decrease of Mg^{2+} vacancies compared with the concentrations of Mg^{2+} and O^{2-} vacancies before the heat treatment, respectively, resulting a greenish blue emission.

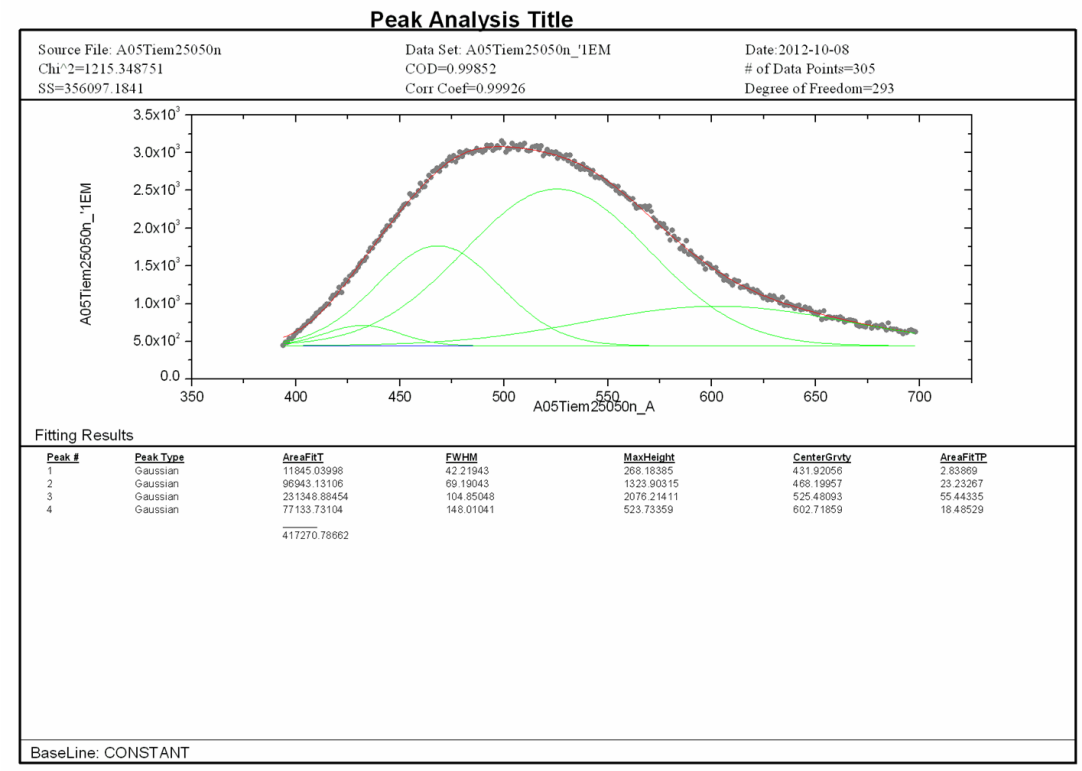

Fig.2-17 Emission spectrum of 0.85mol%Ti doped $MgAl_2O_4$

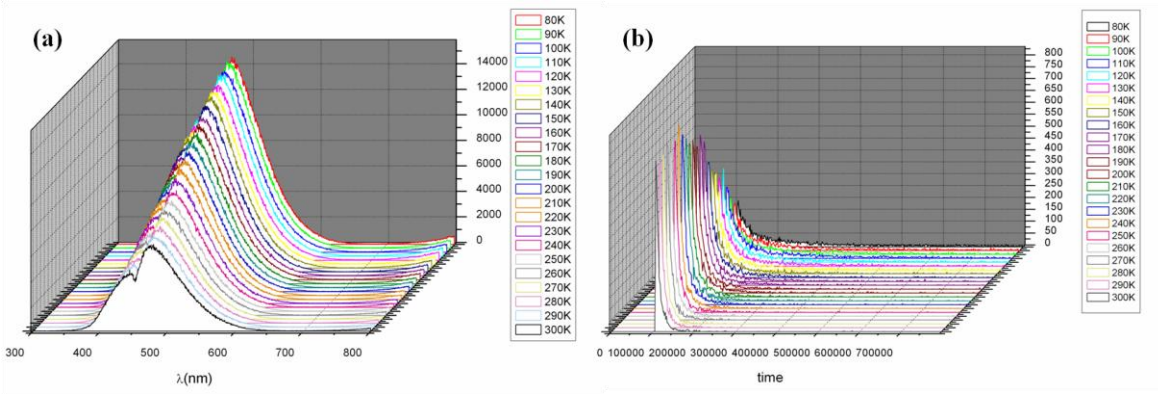

Fig.2-18 (a) PL result from 80K to 300K, (b) Decay time curve from 80K to 300K

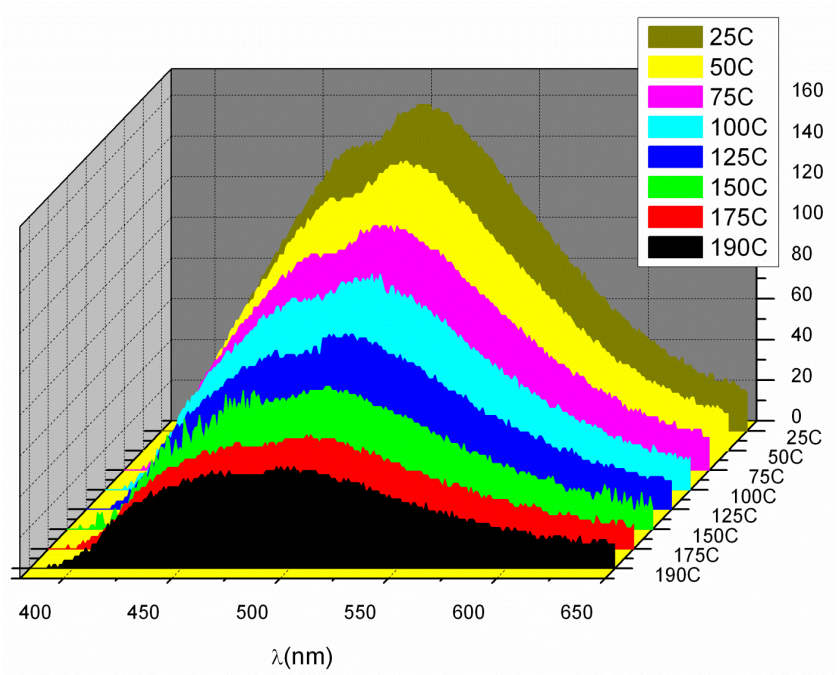

Fig.2-19 Thermal quenching from 298K to 463K

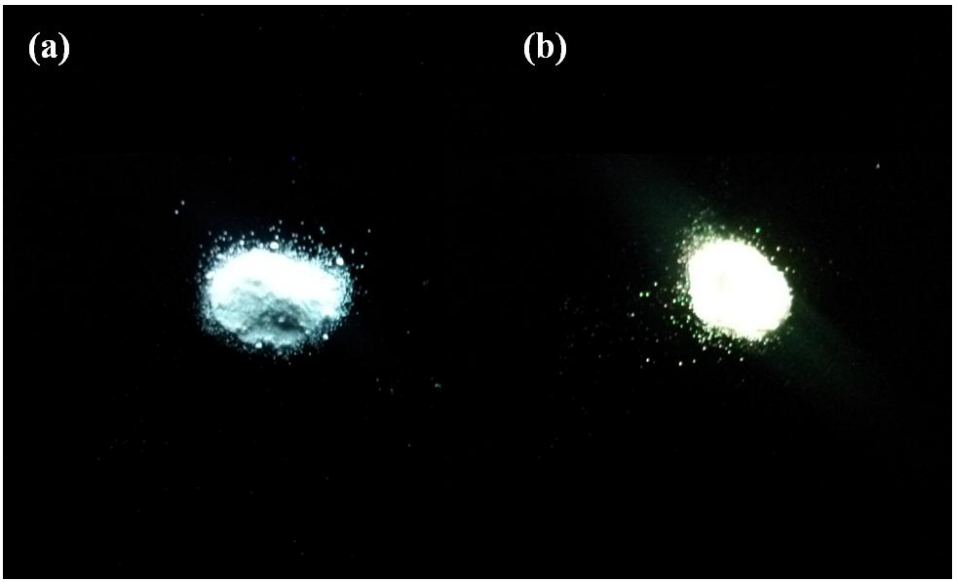

Fig.2-20 White emission of Ti doped $MgAl_2O_4$ and yellow emission of commercial phosphor

Fig.2-16(a) shows a prediction of emission peak changed by reduction condition. The difference between previous Fig.2-15 is related to Ti^{4+} peak which has decrease in tendency in comparison to oxidation condition as Ti^{4+} has tendency to convert into Ti^{3+}. After reduction process, intensity of emission peaks at 490nm and 620nm related to Ti^{4+} decreases as well as the relevant intensity of peak and hence decrease in overall emission width. On the other hand, in spite of reduction condition, such single crystal of similar peak as Fig.2-16(b)[9] is expected to form as Ti^{4+} will not completely eliminated.

In case of 1.7mol%Ti doped $MgAl_2O_4$, the contribution of Ti^{3+} is confirmed in emission spectrum. The emission of 440 and 550nm, which mainly comes from Ti^{3+}, is analyzed by area fraction. As the result, the contribution of Ti^{3+} is obtained about 40%. On the other hand, 1 to 5 ratio of Ti^{3+} and Ti^{4+} was taken by XPS result. These differences are caused by two reasons. Firstly, the ratio of Ti^{3+} and Ti^{4+} is not contributed to emission as the same efficiency. Secondly, 490nm emission is majorly affected by Ti^{3+} and also Ti^{4+} is weakly contributed to 550nm emission according to DV-Xa calculation. So, it cannot be matched perfectly. In spite of these differences, DV-Xa calculation and experimental result are well supporting the existence of Ti^{3+} and Ti^{4+}.

Emission result of 0.85mol%Ti doped $MgAl_2O_4$ is shown in fig.2-17. Emission spectrum is separated by 4 peaks(430, 470, 525 and 600nm). Correlationship factor is matching above 99.8%. 4 peaks show the tendency of blue shift compare to 1.7mol% Ti doped $MgAl_2O_4$. However, total emission peak does not show big

difference. Also, the strongest intensity is observed at 525nm. Similarly, Ti^{3+} and Ti^{4+} in emission are differently contributed compare to XPS result aspect of quantitative result.

PL and decay time was observed in terms of temperature from 80K to 300K whether other energy route can be existed or not. This is the result for more detailed analysis. According to PL and decay time curve in fig.2-18, thermal quenching was confirmed and decay time decreased as increasing temperature. It indicates that non-radiative transition rate increased and this phenomenon was thermally activated. Eventually, other energy transfer route cannot be confirmed. Therefore, the emission mechanism can be agreed from experimental results and calculations.

The thermal quenching is depicted in fig.2-19 from room temperature to 463K(~190^{o}C). Heat is produced applying phosphor characteristic using UV-LED chip for the application and as result of heat production emission property is reduced. Similarly, our result also shows well known decrease in emission property from thermal quenching.

Commercial phosphor(무진, MUJIN global) of $(Ba,Sr,Ca)_2SiO_4:Eu^{2+}$ is obtained to compare the brightness efficiency for UV-LED. 365nm excitation is used for commercial phosphor which is classified as silicate phosphor. The brightness is compared under 250nm excitation because Ti doped $MgAl_2O_4$ does not emit at 365nm excitation. Fig.2-20(a) is Ti doped $MgAl_2O_4$ and (b) is a commercial phosphor. A strong white emission can be observed from Ti doped $MgAl_2O_4$ whereas commercial phosphor shows yellow emission. Superior sample aspect of

brightness cannot be distinguished. However, commercial phosphor is optimized to 365nm excitation. In this way, commercial phosphor can be considered.

2.5 Conclusion

In this work, we studied white emission from Ti-doped spinel phosphor. These emission characteristics were explained using energy diagrams of first-principle program, DV-Xα. In contrast to blue emission from most Ti-doped single crystal $MgAl_2O_4$, Ti-doped $MgAl_2O_4$ powder exhibited white emission. It is ascribed to high concentrations of Mg^{2+} and O^{2-} vacancies in the powder samples. The emission peak was found to consist of four deconvoluted peaks, of 442, 490, 545, and 616 nm, from synthesized powder under excitation at 250 nm. From DV-Xα calculations, Ti^{3+} in tetrahedral sites and Ti^{4+} in octahedral sites were found to contribute to greenish blue emission at 490 and 545 nm, which were strong and broad. The red emission at 620–710 nm was produced by high concentration of Mg^{2+} and O^{2-} vacancies in the powdery spinel. Some discrepancies in the emission wavelengths must be caused largely by the cluster size, i.e., larger energy separations, and partially by the limitations in modeling electron vibrations (modes), electron relaxation and nuclear transition in the excited state as discussed above. The Ti-doped $MgAl_2O_4$ phosphor was found interesting because it does not use rare earth elements and can provide white emission using a single host material[27].

Part.3. A study on Ti doped nano $MgAl_2O_4$ phosphor

3.1 Introduction

When the bulk sized material changes into the nano sized material, its material properties, such as mechanical, optical, electrical property and so on, changes.[28-33] These changes of properties attract attention to the study of nano materials as a design for materials. Like previously mentioned, this phenomenon affects the study of phosphor in nano size aspect of emission property.

Depending on the sizes of nano particle, it can be broadly explained according to three following regimes. Firstly, the ordinary sizes showing in the range between dozens of nm to hundreds of nm. In this range, no big difference is observed but the emission properties are often reduced due to relatively small sized because of defects.[34-35] Secondly, when the material size approaches to de Broglie wavelength, the energy band gap of material is increased due to quantum confinement effect. From this tendency, emission color is able to be tuned. Hence, the quantum dot is actively studied. Thirdly, when the size is smaller than de Broglie wavelength, the characteristic of atoms is relatively high compare to other regimes. So, this range of sub nm, known as “super atoms” or “atomic cluster”, have been studied widely.[36-39]

A change of emission property is observed in nano phosphor due to doping site as

well as quantum confinement effect as described in 2nd regime.[12,40] Generally, a charge valence of dopant and a doping site affect emission properties in phosphor. Hence, dopants can be located in additional doping site like surface except for other usual sites in nano phosphor. Moreover, one of the defects supplies surface which normally does not generate occupation of dopant in bulk system. A variety of emission phenomena by occupation site, which is occasionally relate to some defects, have been reported.[12,40] According to some reports, $MgAl_2O_4$ among nano phosphor was successfully synthesized by sol-gel, hydrothermal and combustion methods. Mn, Tb and Eu were considered as dopants.[4,41] In case of Mn doping, emission at 519nm was detected with excitation at 278nm in bulk $MgAl_2O_4$ but emission at 650nm was detected by excitation at 290nm in case for nano sized system. Also emission intensity was improved as increasing Mn contents(0.1~2mol.%) in bulk system. However, emission intensity in nano system shows the opposite tendency.[4] These $MgAl_2O_4$ powders were obtained about 40~50nm size distribution and it was synthesize through relatively higher temperature.[41-42] In spite of many kinds of nano $MgAl_2O_4$ synthesis, Ti doped nano $MgAl_2O_4$ have not been reported. Recently, our team has successfully synthesized Ti doped nano $MgAl_2O_4$ to compare with bulk system.

3.2 Sample preparation

$Mg(NO_3)_2 \cdot 6H_2O$(Aldrich, Mg nitrate), $Al(NO_3)_3 \cdot 9H_2O$(Aldrich, Al nitrate) and $CO(NH_2)_2$(Aldrich, Urea), $C_{10}H_{14}O_5Ti$(Aldrich, Ti oxy-acetyl-acetonate) is used for start materials. The ratio of Mg nitrate and Al nitrate maintains 1:2 mole fraction to get $MgAl_2O_4$ and x mol.% Ti oxy-acetyl-acetonate is mixed with Mg nitrate and Al nitrate in DI-water. All the powders dissolved in DI-water for homogenization and then followed by evaporation of water on a hot plate. The mixture is fired at 500^oC and 1000^oC for 1h in oxidation atmosphere after evaporation of water. The phases of synthesized powder is analyzed by X-ray diffractometer(XRD, Rigaku) and emission properties are measured by fluorescence spectrophotometer(PSI, PL Darsa pro-5000 system). Xe lamp at 250 and 360nm excitation is used for light source during PL measurement. Oxidation states of Ti ions were analyzed using X-ray Photoelectron Spectroscopy (XPS, Sigma probe, ThermoVG, UK). Powder morphology and size is observed by high resolution TEM(transmission electron microscopy, JEOL, JEM-2100F). And Ti doping site and Mg^{2+} vacancy are also detected from high resolution STEM(Scanning transmission electron microscopy) images.

3.3 Results

The fig. 3-1 shows XRD result for Ti oxy acetyl acetonate. The powder was prepared at 500^{o}C and 1000^{o}C-1h in air. The synthesis of TiO_2 is predicted to form after heat treatment at high temperature without urea because TiO_2 is the most stable phase among Ti_xO_y species although urea is well known for combustion fuel. From XRD results, Ti oxy acetyl acetonate is converted to anatase phase of TiO_2 at 500^{o}C and rutile phase shows up at 1000^{o}C. TiO_2 phases consist of 3 phases which is anatase, brookite and rutile. Anatase phase is known to be stable at low temperature and the stability of rutile needs higher temperature. It indicates that Ti doped nano $MgAl_2O_4$ can be easily obtained below 1000^{o}C if the temperature range can be overlapped with the synthesis of nano $MgAl_2O_4$ with phase transition to TiO_2.

Meanwhile, nano $MgAl_2O_4$ can be taken by 1 to 1 ratio of MgO and Al_2O_3. Combustion method is well known for the synthesis of $MgAl_2O_4$ from Mg nitrate, Al nitrate and urea.[4,41] Mg nitrate and Al nitrate plays a role as an oxidizing agent and urea is used as reducing agent forming redox reaction during synthesis.

Fig.3-2 is the XRD results of $MgAl_2O_4$ at 300^{o}C and 1000^{o}C. In case of heat treatment at 300^{o}C, the broad peaks appear due to low crystallinity. However, all the peaks are accurately matched with $MgAl_2O_4$ phase. The peak near 23^{o} degree appeared because of ethanol effect for fixing powder on XRD holder.

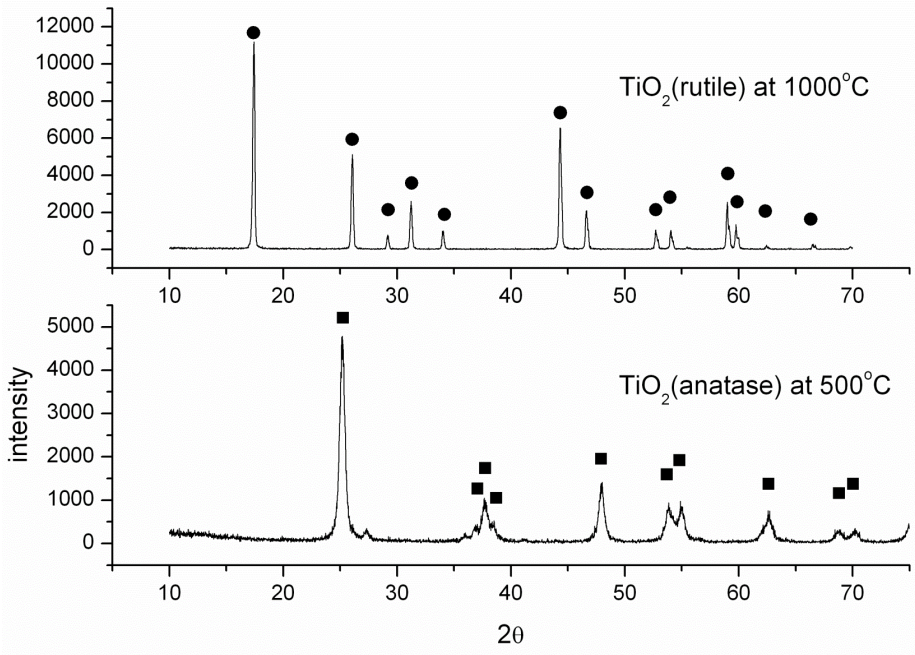

Fig.3-1 the XRD results of Ti oxy-acetyl-acetonate at 500°C and 1000°C-1h

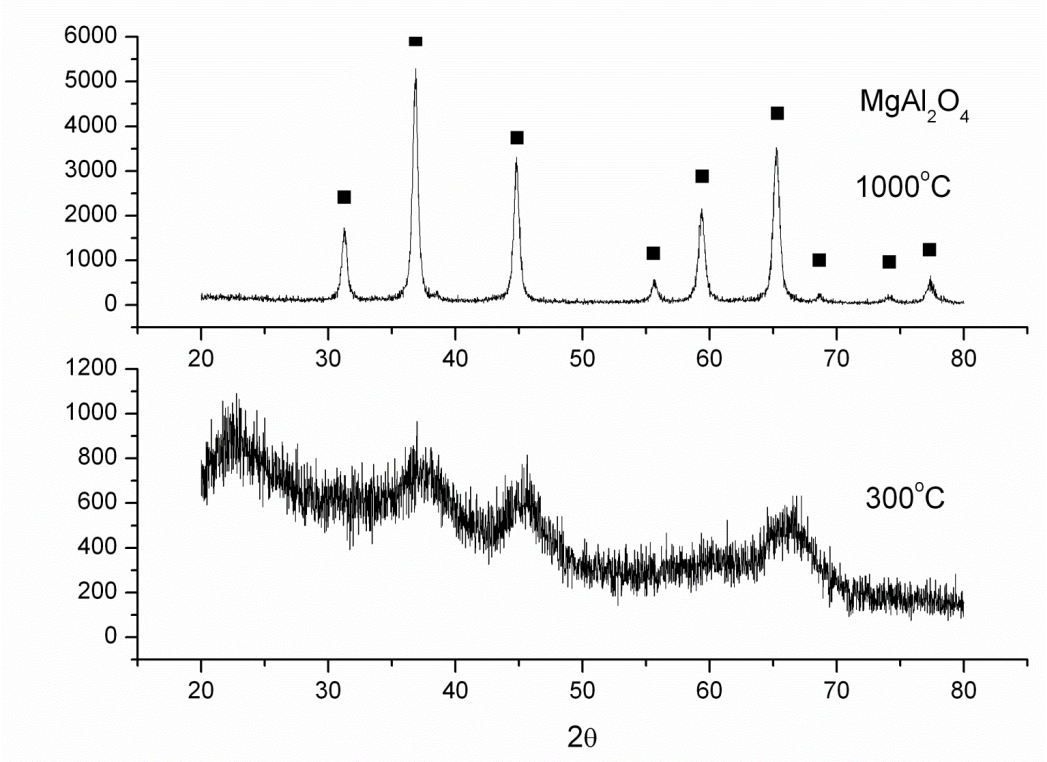

Fig.3-2 the synthesis of nano $MgAl_2O_4$ at 300°C and 1000°C-1h

On the other hand, the synthesis at 1000°C is perfectly corresponded to the $MgAl_2O_4$ phase without any secondary peak. According to our research, $MgAl_2O_4$ can be synthesized at 500°C but poor crystallinity is obtained like the synthesis at 300°C. As already mentioned, $MgAl_2O_4$ normally needs 1 to 1 ratio of MgO and Al_2O_3. In spite of that condition, $MgAl_2O_4$ can maintain a wide range of non stoichiometry at high temperature. In this point of view, it seems that non stoichiometry spinel can be obtained from combustion method.

Aspect of the stability of non stoichiometry, $MgAl_2O_4$ can easily generate intrinsic defects. Mg^{2+} vacancy is the most well known example of intrinsic defect as we dealt in part.4. Generally, Mg^{2+} vacancy causes red emission.[8-9] It predicts that the defect is more activated with nano size.

Fig.3-3 deals with emission result for pure $MgAl_2O_4$ which synthesized at 1000°C. Emission peak is confirmed near 730nm under 250nm excitation due to Mg^{2+} vacancies. This result corresponds to the results of other researchers.[9] Ti oxy acetyl acetonate is reacted with Mg nitrate, Al nitrate and urea in DI-water for Ti doping. It is purposed for homogeneity reaction by ionization. As we discussed, $MgAl_2O_4$ can be synthesized at 300°C from fig.3-2. But Ti doped nano $MgAl_2O_4$ does not show any emission due to unclean surface by remaining organic on surface.

XRD result is derived for 2mol.% Ti doped $MgAl_2O_4$ from fig.3-4. As confirmed, Ti doped $MgAl_2O_4$ is synthesized at 500°C and 1000°C and any contamination was not observed on surface.

Low crystallinity peak is observed at 500^{o}C. In contrast, clean and high intensity are taken at 1000^{o}C because 500^{o}C is not enough to grow the particle compare to 1000^{o}C. Moreover, TiO_2 segregation does not show up as a secondary phase. According to previous study about Ti doped bulk $MgAl_2O_4$, Ti does not segregate at 8.5mol doped case. PL result for synthesis at 500^{o}C is shown in fig.3-5. The bluish white emission occurs at 250nm excitation and this tendency is similar to the emission in bulk system but emission color is slightly shifted to blue in nano. As one of the possibility, it can be inferred that band gap increases as size decrease from bulk to nano size. It can affect to blue shift of emission.[43-44] Another possibility is the increase in relatively ratio of Ti^{3+} between Ti^{3+} to Ti^{4+} compare to bulk system and because of existence of strong emission at 720nm even after Ti doping. Normally, 720nm emission is eliminated by Ti^{4+} in Al site due to compensation.[9] Likewise, 620nm emission about Schottky pair, which is generated from Ti^{4+} in Mg site, is weaker than in bulk system.

An interesting factor is discovered from emission result of Ti doped nano $MgAl_2O_4$. Like bulk system, emission peak is deconvoluted to 4 peaks by 4 cusps which match 425, 480, 525, 610nm emission. But it seems that mechanical noise appears at these 4 positions due to relatively low intensity. In spite of low intensity, it expects that overall emission mechanism has to be the same as bulk system because peak shape and emission color is similar to that of bulk.

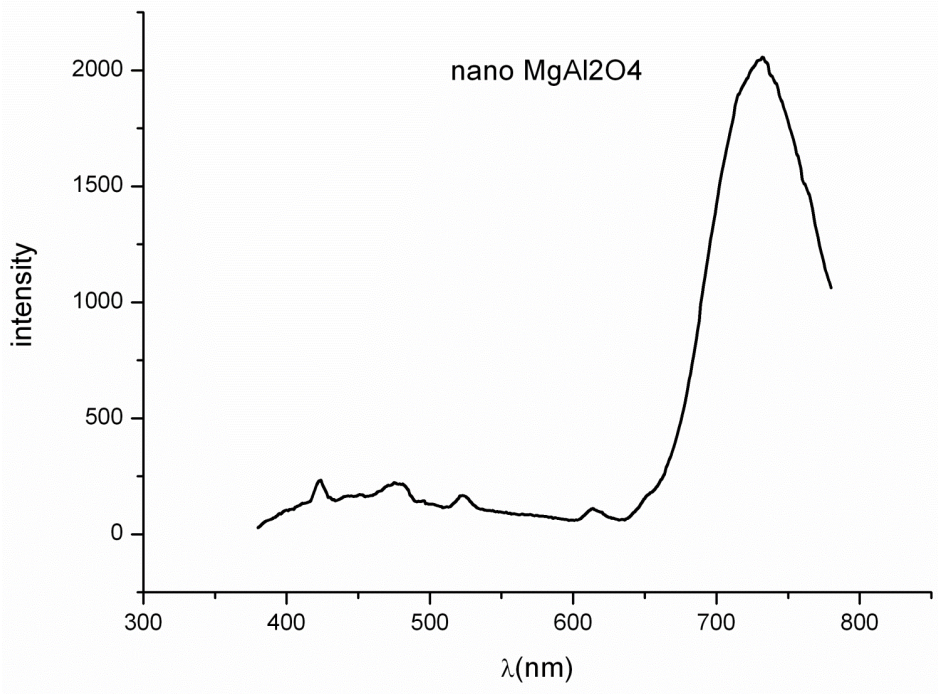

Fig.3-3 Emission of pure nano $MgAl_2O_4$ by intrinsic defect at 250nm excitation

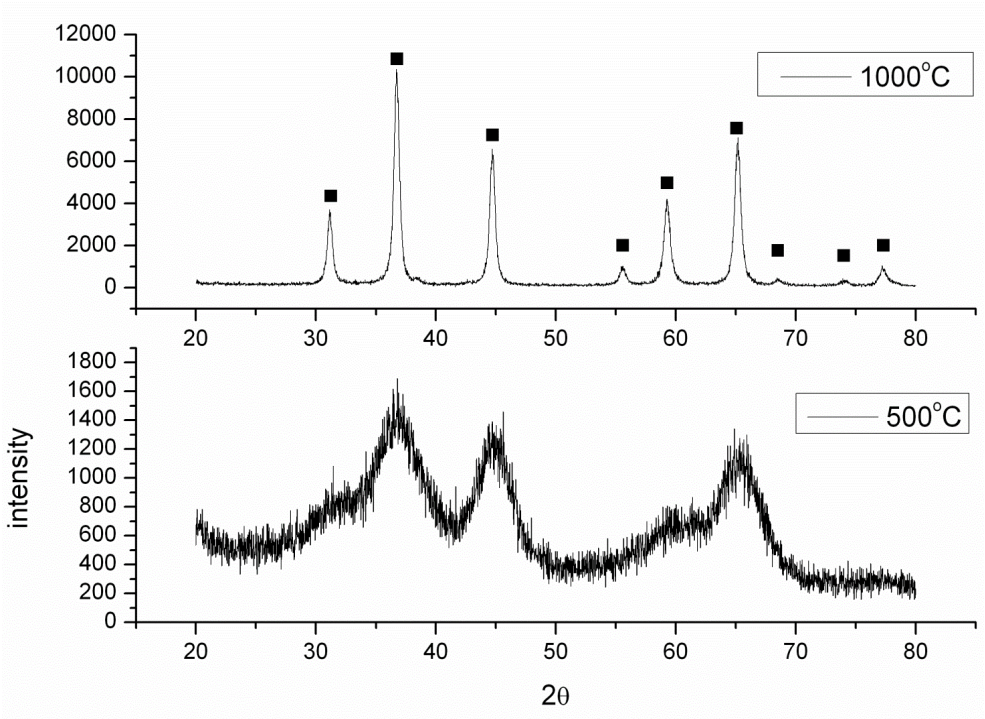

Fig.3-4 XRD results of 2mol% Ti doped nano $MgAl_2O_4$

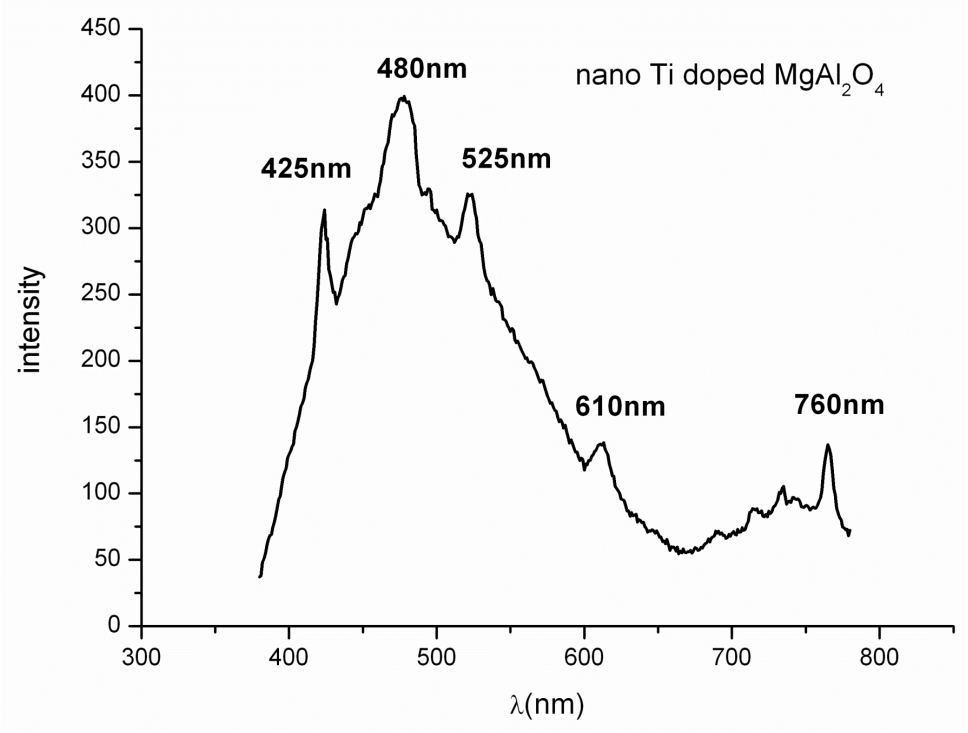

Fig.3-5 Emission result of 2 mol.% Ti doped nano $MgAl_2O_4$ at 250nm excitation

Meanwhile, 760nm emission is also detected about intrinsic defect as judge by inference in spite of Ti doping. These imply that Ti^{3+} was dominantly occupied in nano $MgAl_2O_4$ unlike in bulk system because 720nm emission about Mg^{2+} deficiency is eliminated by Ti^{4+} in octahedral site.[9] Additionally, it seems that Ti ions can be occupied in tetrahedral site as well as octahedral site according to similar white emission. The chromaticity coordinates of Ti-doped nano $MgAl_2O_4$ powder are presented in 1931 CIE diagram, shown in Fig. 3-6, as a comparison of nano and bulk systems. The result supports to blue shift from bulk to nano.

Meanwhile, emission property is observed under 360nm excitation in case of 2 mol.% Ti doped nano $MgAl_2O_4$ which prepares at 500^{o}C-1h as shown in fig.3-7. However, no emission is confirmed at 360nm excitation among 0.2 and 1 mol.% Ti doped case. Also the emission is not detected under 360nm excitation by synthesis at 1000^{o}C-1h in case of 2 mol.% Ti doped nano $MgAl_2O_4$. The charge valency and doping site are strongly related to emission property as important factors.

In order to detect the charge valence, nano 2mol.% Ti doped $MgAl_2O_4$ is measured by XPS. The binding energy between Ti and near atoms shows along X-axis in fig.3-8. The results of synthesis temperature at 500 and 1000^{o}C are derived in fig.3-8(a) and (b), respectively. As already mentioned, bluish white emission is obtained at 360nm excitation. This phenomenon is related to Ti ions on the surface at Mg site as well as Al site. Actually, many results have been reported that the surface is one of the most important factors for emission property.[12]

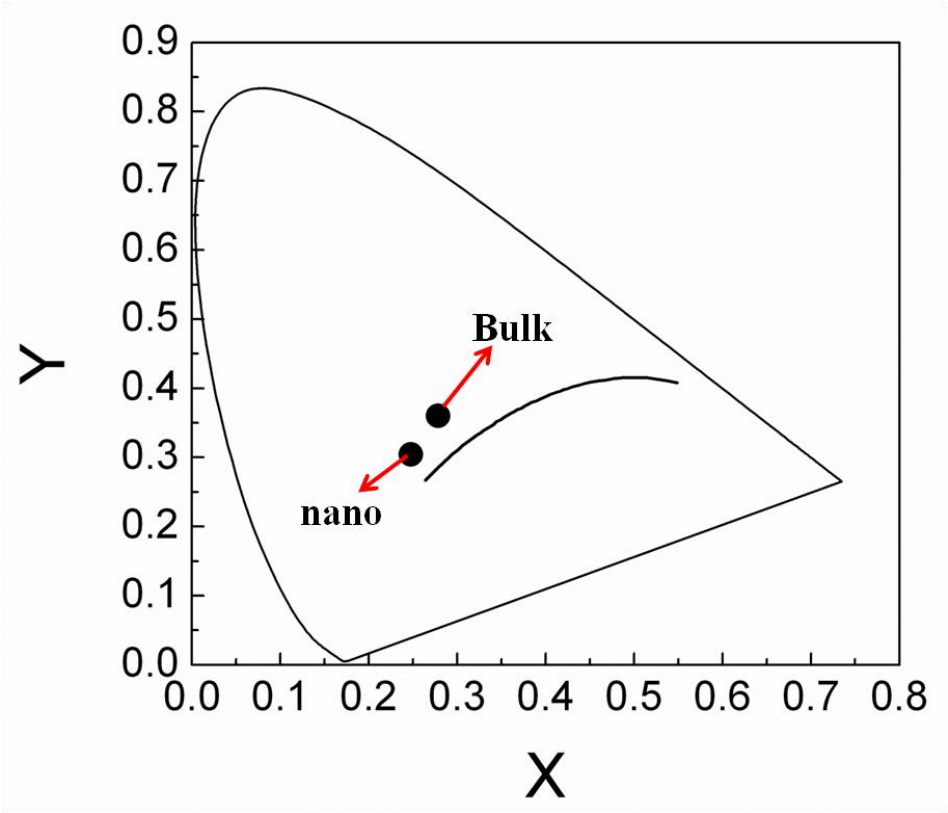

Fig.3-6 Chromaticity coordinate(nano and bulk)

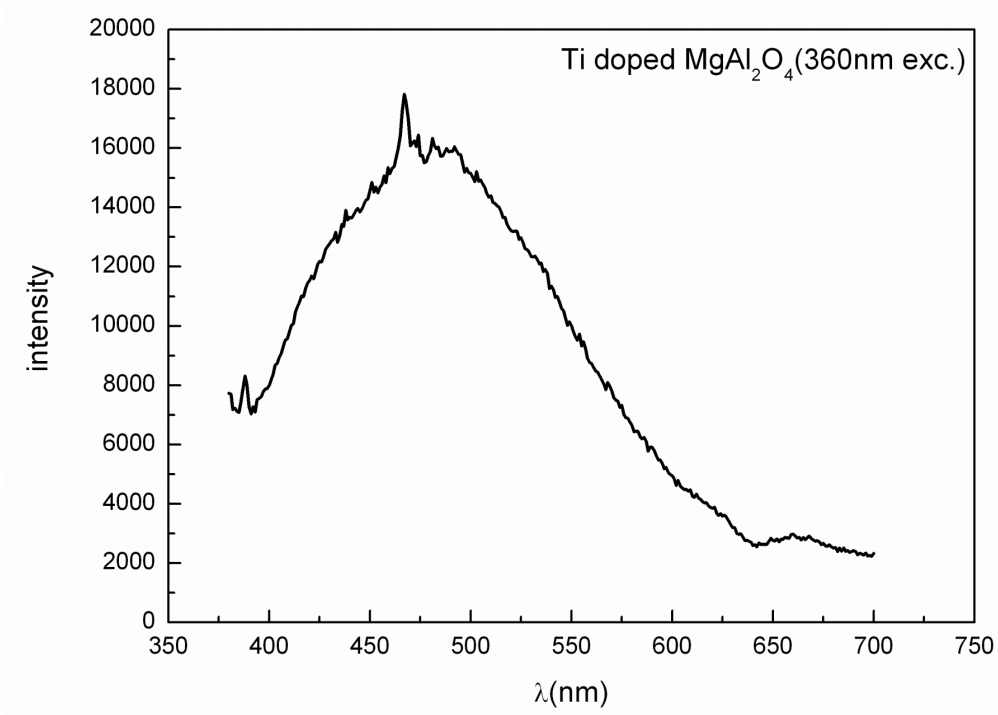

Fig.3-7 Emission result of 2 mol.% Ti doped nano $MgAl_2O_4$ at 360nm excitation

Meanwhile, Ti^{3+} ion shows up as dominant phase among Ti ions regardless of synthesis temperature. In case of bulk system, Ti^{4+} ion is confirmed as a main phase by XPS. In contrast, nano Ti doped $MgAl_2O_4$, the blue shift of emission is well explained by increase in ratio of Ti^{3+}. The overall blue shift occurs due to relatively reduced number of Ti^{4+}. However, it implies that Ti^{3+} as main phase draws attention to this result because powder is synthesized by oxidizing atmosphere. Also the location of Ti^{3+} is maintained at the same position without any change but Ti^{4+} shows a different tendency. It seems that Ti^{4+} of the powder, which is synthesized at 500^{o}C, is shifted to low bind energy but not at 1000^{o}C. It predicts that some of Ti^{4+} ions are existed on the surface and Ti^{4+} ions on the surface are weakly bonded with other atoms compare to Ti^{4+} in the crystal. And two broad Ti^{4+} peaks are shown on both of the sides of 458.5eV but both of the peaks are hard to distinguish each other because the existence of broad peak comes from a low crystallinity. And it expects that two peaks are related to doping site like on the surface and inside the crystal. Meanwhile, it is supposed that Ti^{4+} is mainly observed at the surface because surfaces are more easily in contact with oxidizing atmosphere. The XPS results support well the presence of Ti on the surface.

Ti doped nano $MgAl_2O_4$ has a long decay time compare to bulk system, but the reason is not clear. The decay time curve is shown in fig.3-9. Decay time is about 55.2μs.

Ti doped nano $MgAl_2O_4$ shows a low luminous intensity compare to bulk system. The color rendering property of nano system(80) is higher than in bulk system(69). As previous emission result in fig.3-5, it can assume that emission mechanism in nano is similar to that in bulk. The existence of Ti^{3+} and Ti^{4+} is confirmed from XPS result. According to our previous result and other reports, Ti ion in octahedral site can be explained and also emission mechanism can be described by our calculation through 1^{st} principle. According to our calculation results in part.2, it expects that the previous calculation can reflect Ti doped nano $MgAl_2O_4$ because the cluster size in calculation set as 2 nm. In the same vein, Ti^{3+} or Ti^{4+} in tetrahedral site generates additional Mg^{2+} vacancy due to charge neutrality. In order to prove this speculation, Ti doped nano $MgAl_2O_4$ is observed by HR-STEM. The original images are submitted in fig.3-10.

Each atom can be distinguished by bright spot in fig.3-10. A STEM image is commonly reflected by z-contrast of atoms. Hence, heavy elements shows brighter image due to intense contrast. For more detail, the contrast intensity is converted to color changes in HR-STEM image as shown in fig.3-11.

Fig.3-11 shows HR-STEM image in (b) and magnified image in (a). As confirmed, Mg atoms arrange at regular distance from fig.3-11(a). The distance between two Mg atoms is measured as 0.2057nm. This value is well matched with $MgAl_2O_4$ (200) plane. According to atomic arrangement, a relatively dark point can be detected among the spot of Mg atoms in fig.3-11. So, this dark point regard as Mg^{2+} vacancy.

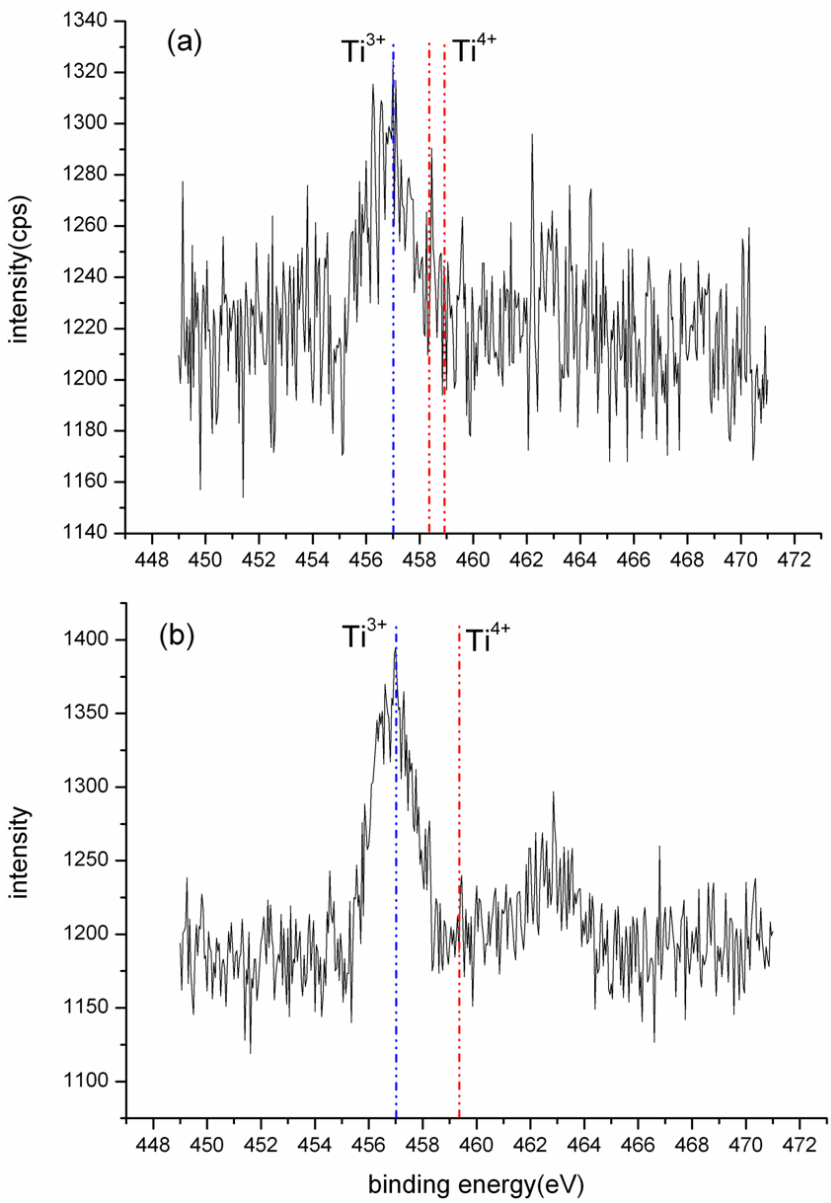

Fig.3-8 XPS results about nano Ti doped $MgAl_2O_4$(a: synthesis at 500^oC, b: 1000^oC)

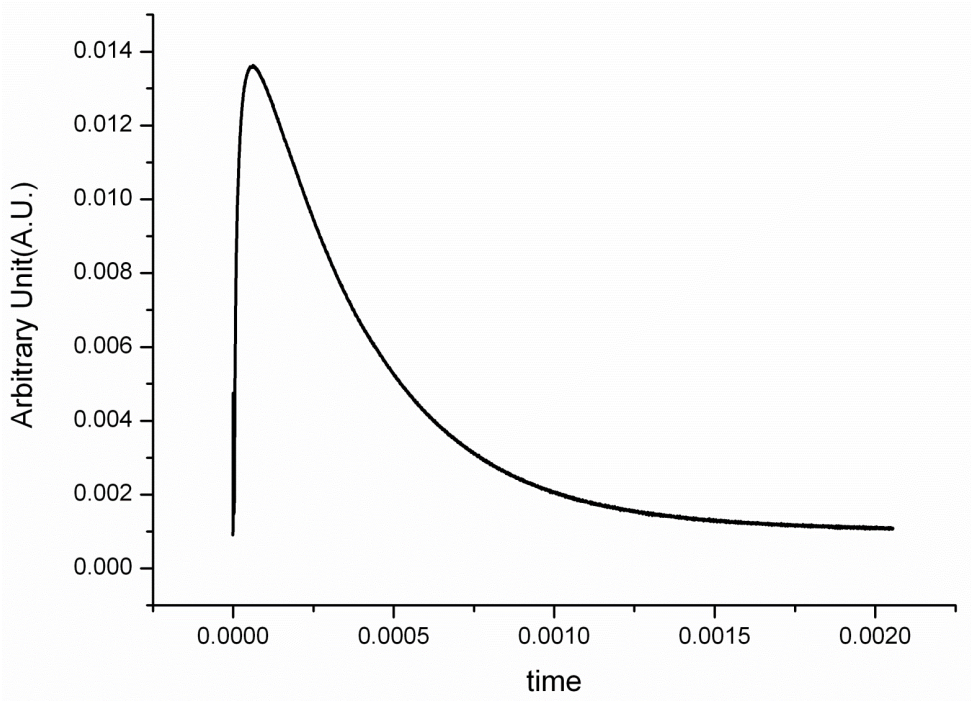

Fig.3-9 Decay time curve of 2 mol.% Ti doped nano $MgAl_2O_4$

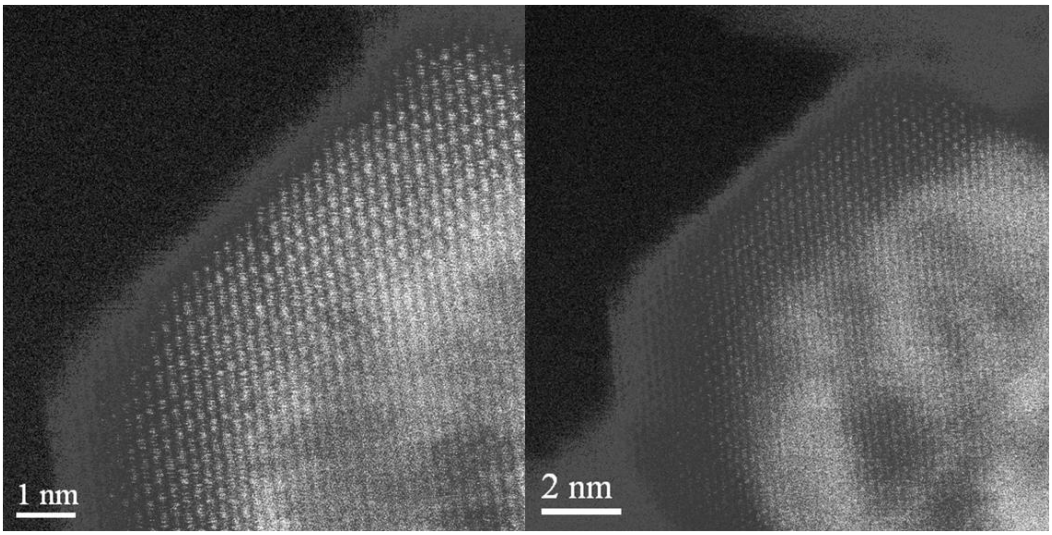

Fig.3-10 HR-STEM original image of 2 mol.% Ti doped nano $MgAl_2O_4$

But this point has also some brightness which is caused by the bottom layer. For more clear understanding, the contrast intensity measurement is shown in fig.3-12.

The contrast intensity shows about atoms inside of red box in fig.3-11(a) as shown in fig.3-12. The contrast intensity of 5^{th} Mg site from left side is lower than that of any other atoms. This result indicates that one atom is missing in Mg site. Meanwhile, other parts are also observed for other reasons for Mg^{2+} vacancy originated in this area.

Fig.3-13 is a HR-STEM image of Ti^{4+} dopant in 2 mol.% Ti doped nano $MgAl_2O_4$. Fig.3-11(a) is a magnified image for selected area in fig.3-11(b). Like fig.3-11, the distance between Mg atom to atom is corresponded to 0.2057nm because this area is located nearby Mg^{2+} vacancy. Outstanding bright atom can be detected in red box unlike fig.3-11. However, Mg and Al atoms cannot be distinguished by z-contrast which is related to atomic number and oxygen cannot be detected due to low atomic number. Therefore, it can guess that a bright atom comes from Ti. Meanwhile, Ti in Mg site causes displacement error because the charge valence and the ionic radius of Ti ions are different from those of Mg^{2+}. So, the displacement error of Ti appears in fig.3-13(a). Aspect of ionic radius, Ti seems big compare to other atoms in fig.3-13(a) because Ti^{3+} and Ti^{4+} of 0.076nm, 0.068nm are bigger than Mg^{2+} of 0.064nm.[45-47]

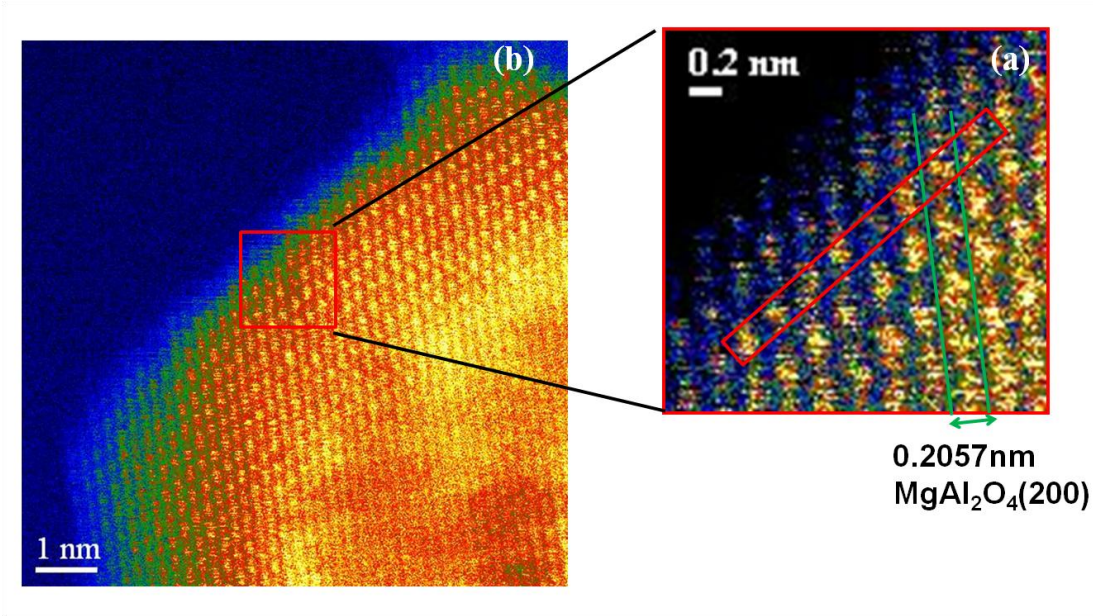

Fig.3-11 HR-STEM image of Mg^{2+} vacancy in 2 mol.% Ti doped nano $MgAl_2O_4$

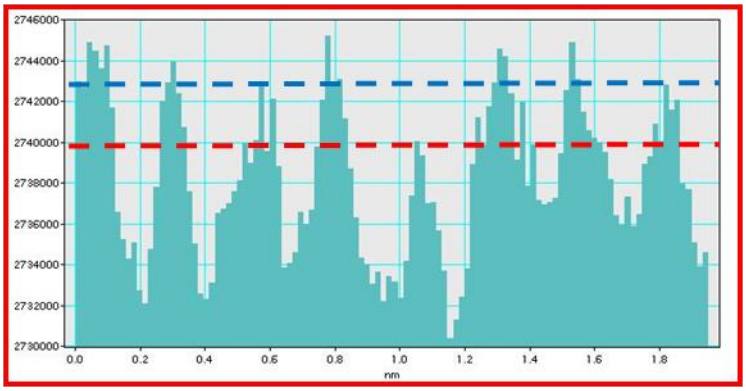

Fig.3-12 Contrast intensity of HR-STEM image in 2 mol.% Ti doped nano $MgAl_2O_4$

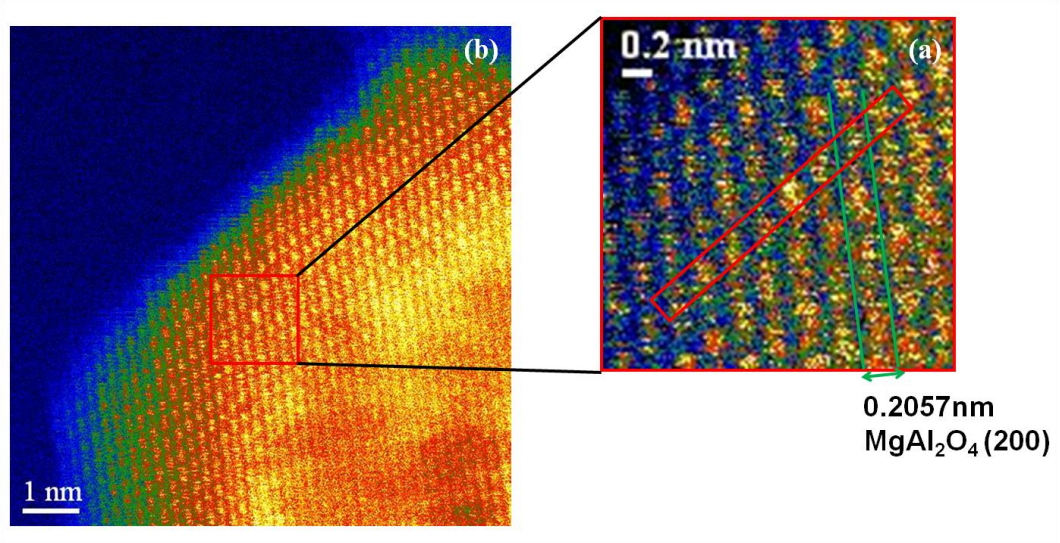

Fig.3-13 HR-STEM image of Ti dopant in 2 mol.% Ti doped nano $MgAl_2O_4$

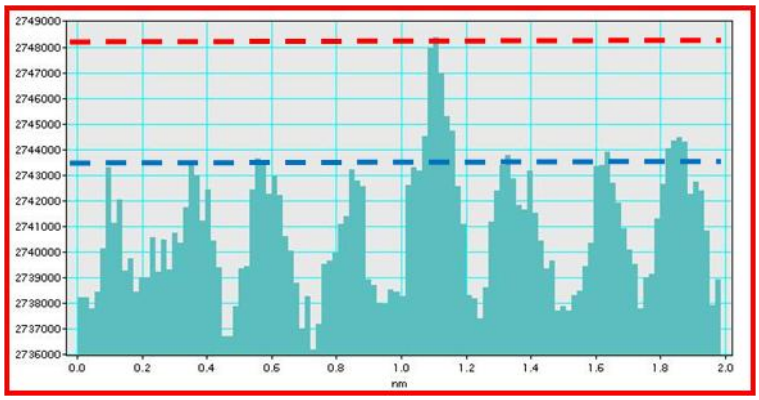

Fig.3-14 Contrast intensity of HR-STEM image about Ti dopant

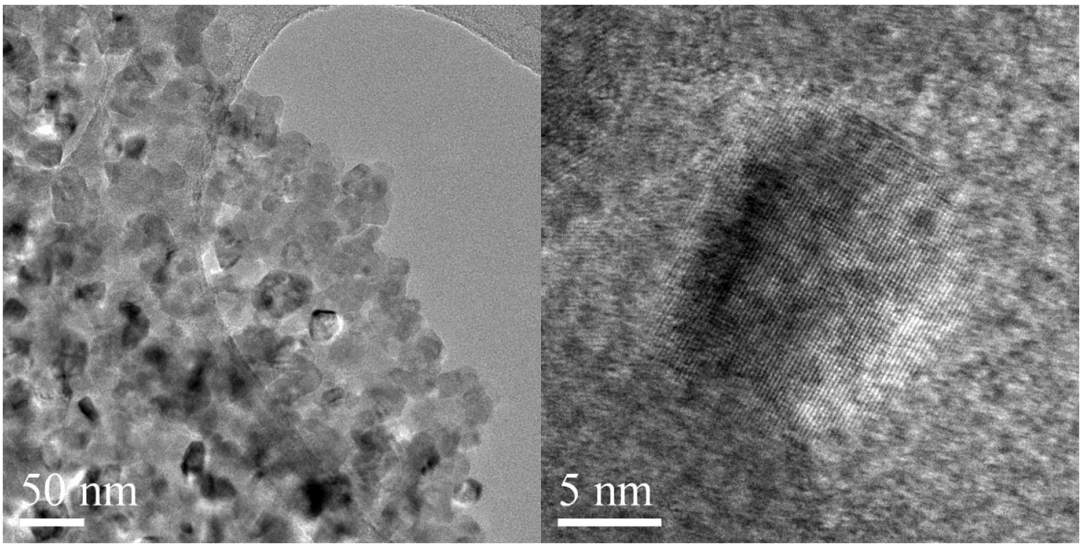

Fig.3-15 HR-TEM image about 2 mol.% Ti doped nano $MgAl_2O_4$

The contrast intensity of Ti doping in Mg site is shown in fig.3-14. Similarly, the contrast intensity of 5^{th} Mg site in fig.3-13(a) from left side is higher than that of any other atoms. And it implies that an element of high atomic number like Ti is occupied in that site. When Mg^{2+} is substituted by Ti^{3+} or Ti^{4+}, Mg^{2+} vacancy is generated due to charge neutrality. But Mg^{2+} vacancy cannot exist in the nearest neighbor because lattice mismatch is reduced step by step. Therefore, it can be predicted that Mg^{2+} vacancy is located in the minimum point of lattice mismatch.

High resolution TEM image about 2 mol.% Ti doped nano $MgAl_2O_4$ at 500^oC can be confirmed in fig.15. Its size is about 20nm. Meanwhile, the crystallite size of 35nm was obtained by Scherrer equation for 2mol% Ti doped nano $MgAl_2O_4$ which was synthesized at 1000^oC.

3.4 Conclusion

Ti doped nano $MgAl_2O_4$ was dealt with a variety of properties until now. $MgAl_2O_4$ from 1 to 1 ratio of MgO and Al_2O_3 was synthesized using Mg nitrate, Al nitrate, Ti acetyl acetonate and urea as starting materials. Nano $MgAl_2O_4$ can be obtained at 300^oC and Ti doping case is shown up at 500^oC. 720nm emission in pure nano $MgAl_2O_4$ is observed by Mg^{2+} vacancy. The bluish white emission at 250nm excitation is obtained by Ti doped nano $MgAl_2O_4$. Like bulk system, the emission spectrum has 4 peak shoulders which are well matched with bulk system. The strong emission spectra, which are caused by Ti^{3+} in tetrahedral and octahedral site, respectively, are detected at 430nm and 550nm among 4 shoulders. And 480nm strong emission is related to Ti^{4+} in octahedral site. Meanwhile, the Schottky pair of Mg^{2+} and O^{2-} vacancies is generated by Ti^{4+} in tetrahedral site which causes the 620nm emission. The 620nm emission of nano system is weaker than that of bulk system. It indicates that the Ti^{3+} in nano system may have increased in ratio between Ti^{3+} and Ti^{4+} compare to the previous in bulk system. Exceptionally, the bluish white emission is observed in 2 mol.% Ti doped nano $MgAl_2O_4$ under 360nm excitation. The powder was synthesized at 500^oC. It seems that some Ti does not make a bonding inside a crystal. Hence, an isolated Ti can be located on the surface aspect of 360nm excitation. The size of synthesized powder is confirmed as 20nm size using TEM. Also the substitution of Ti in Mg site was observed by HR-STEM and Mg vacancy was detected near Ti doping. From this result, the possibility struck for

the existence of Ti in Mg site and Schottky pair. It indicates that HR-STEM study is supported to our previous calculation in bulk system as a meaningful result through experiment. The white emission of Ti doped nano $MgAl_2O_4$ is feasible phosphor as a brief synthesis and bright emission. However, relatively low emission intensity remains as a further work compare to bulk system. In spite of this problem, the potential feasibility is discovered as phosphor for blue LED due to a long excitation compare to bulk system.

Part.4. Greenish emission from poly-crystalline Transparent $MgAl_2O_4$ spinel

4.1 Introduction

Al_2O_3 and $MgAl_2O_4$ attract attention to many research fields due to its outstanding mechanical properties and optical properties. Aspect of optical properties, transmission phenomenon about transparent ceramics has been researched by synthesizing single crystal growth or sintering under high temperature and high pressure. Also, fabrication for laser materials has been studied as host materials because of its excellent luminescent property by additives.[48-50] Furthermore, due to the beautiful appearance characteristic with dopants, it is also used as jewelry.

As explained in previous part, many studies are in progress incluing rare earth doping as well as transition metal doping. Especially, transparency and emission properties are obtained in $MgAl_2O_4$ which is successfully synthesized through Ti, Cr, V, Mn, Ni and Nb doping by single crystal growth according to the latest research.[11] However, there are some problems regarding synthesis of single crystal growth due to the strict conditions requirement and also it is hard to obtain a bigger size compare to other method.

In order to solve this problem, poly crystalline growth can be considered. In case

of poly crystalline growth, it is not difficult to get the optical property but it there are some limitations of transparancy. Some factors disturb transmittance like grain-boundary, pore and impurity.[51-53] Firstly, grain boundary scatters incident ray at grain boundary and it causes transparency degradation, thereby the relationship between grain boundary and transmittance has been researched by many other researchers. Generally, when grain size is smaller than the wavelength of incident beam, grain boundary scattering can be ignored as explained by Snell's law.[53] Grain growth can be suppressed by controlling the sintering schedule or addition of grain growth inhibitor.[54,55]

The use of high purity start materials can avoid existing impurity as scattering factor. On the other hand, pore can be partially removed with heating schedule and pressure but perfect elimination cannot be achieved. Hence, pore is considered as the most important factor for transmittance. Despite unstable pore control, transmittance of transparent $MgAl_2O_4$ can be approached to that of glass using HP(hot press), HIP(hot isostatic pressing) and SPS(spark plasma sintering) under high temperature and pressure according to literature survey.[56-60]

Meanwhile, white emission of Ti doped $MgAl_2O_4$ is observed by synthesis in air according to our previous results.[15] According to Sato et al., Ti doped $MgAl_2O_4$ by single crystal growth shows blue emission, whereas, our white emission is worthy of notice. [9]

However, poly crystalline transparent phosphor of $MgAl_2O_4$ is not reported. Therefore, this study deals with transmittance and emission property through

sintering under high temperature and pressure.

4.2 Sample preparation

In this research, samples were prepared using commercial $MgAl_2O_4$(TSP-20, Taimei Chemicals Co. Ltd., Nagano, Japan, purity: 99.9%) and TiO_2(Nanotek, USA, purity: 99.95%). 0.17, 0.85, 1.7mol% Ti was used as a dopant in $MgAl_2O_4$. The powder was mixed in ethanol at 2000rpm-30min without ball for homogeneity then synthesized at 1000°C-2h in air.

From obtained powder, 0.6gram was sintered in graphite mold, which has 10Φ diameter, by SPS(spark plasma sintered, SPS-1050, Sumitomo) in vacuum. The sintering temperature varied from 1150°C to 1300°C for 20min. The pressure of sintering condition was fixed at 80MPa with heating rate of 20°C/min. After sintering, both of the sample surfaces were grinded, with 6μm and 1μm, then polished for mirrored surfaces. Transmittance and reflectivity were measured by transmission spectroscopy(SolidSpec-3700DUV, JEOL, Japan) in the range between 200nm~1600nm. For micro structure observation, the sample was cross-sectioned, then thermal etched under 100℃ lower temperature than previous sintering temperature. Microstructure images were observed by field emission-scanning electron microscopy(FE-SEM, Hitachi, Japan) and transmission electron microscopy(TEM, JEOL, Japan).

4.3 Results

The Fig.4-1 shows the in line transmission results of Ti doped $MgAl_2O_4$, which sintered at 1300°C-20min, 0.17 0.85 and 1.7mol% Ti were selected as Ti contents. Transmittance shows a decrease in tendency with increasing Ti contents. On the other hands, transmittance was improved by doping Ti up to 1 mol% according to other report.[9,62] However, in case of single crystal growth, Ti doped $MgAl_2O_4$ was reported that these tendencies were related to reduction in intrinsic defect of Mg^{2+} vacancy by compensation of Ti doped $MgAl_2O_4$ as a single crystal. It also has a limitation of Ti contents. Over addition of Ti content into $MgAl_2O_4$ shows drops in transmittance. But the compensation of Mg^{2+} deficiency does not significantly affect the improvement of transmittance because poly crystalline Ti doped $MgAl_2O_4$ has many kinds of defect. For this reasons, it appears that 1.7mol% Ti doped $MgAl_2O_4$ has a no transmittance property.

Meanwhile, the transmittance drop occurs in red region within visible range. The single crystal of transition metal doped spinel also shows the same tendency.

As related to this transmission phenomenon, the change of apparent color was discovered as other outstanding characteristic. The photograph image shows that the apparent color of sintered body is converted to blue as shown in fig.4-2. It seems that the drop in transmittance in red range affects the change of apparent color.

In the case of reducing sintering temperature to 1250°C, the sintering characteristics are different from that of 1300°C. In-line transmission of sintered

sample at 1250°C deals in fig.4-3. Aspect of transmittance, 0.17mol% Ti doped $MgAl_2O_4$ is better than undoped case. This characteristic correspond to single crystal Ti doped $MgAl_2O_4$. As we already mentioned, the transmittance improvement has been explained with Ti doping which compensates Mg^{2+} deficiency in $MgAl_2O_4$.[9] However, the reason for the improvement of transmittance is different compare to single crystal. In our system, Ti helps to get the good sinterbility. So, this reason is more encouraged. The sinterbility becomes better and better with increasing Ti contents.

The sample edge does not sinter except 1.7mol% Ti doped $MgAl_2O_4$ as shown in fig.4-4. This result is an evidence to support increase in sinterbility by addition of Ti. And also this result is well matched with previous result about 1300°C sintered sample. In case of SPS(spark plasma sintering), the sample edge normally obtains higher temperature compare to the inside because a sample is sintered through graphite mold by the electric current. Eventually, it supposes that vacancies are actively generated at sample edge by temperature gradient of sample because of relatively high temperature. This phenomenon, which is normally observed in transparent ceramics at high temperature and high pressure, is related to decrease in transmittance.

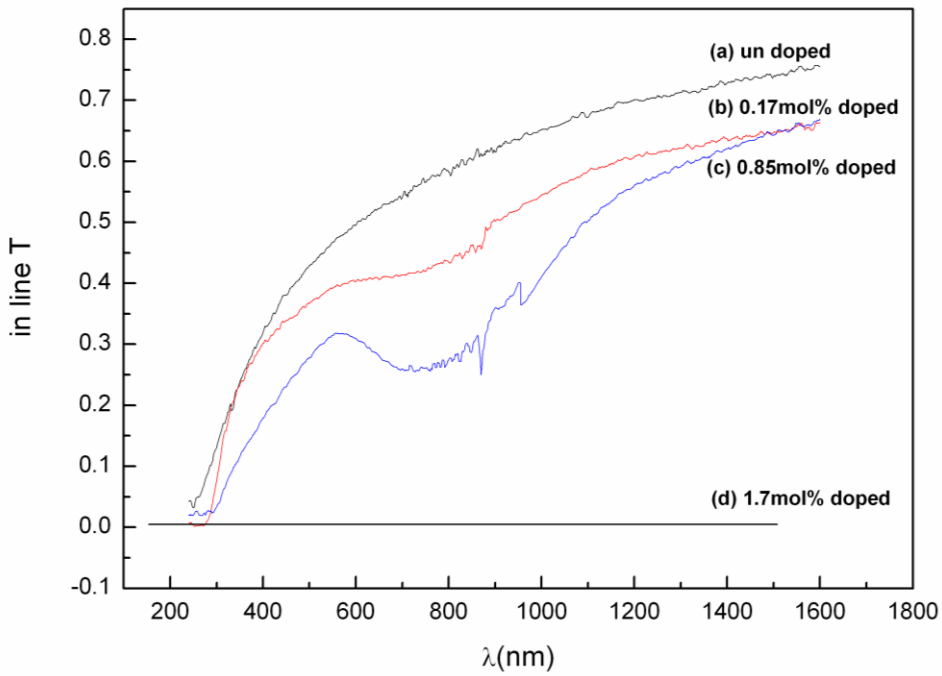

Fig.4-1 In-line transmission result of Ti doped $MgAl_2O_4$ at 1300℃-20min

Fig.4-2 The sintered body at 1300℃-20min about x mol% Ti doped $MgAl_2O_4$: (a) 0.17mol%, (b) 0.85mol%

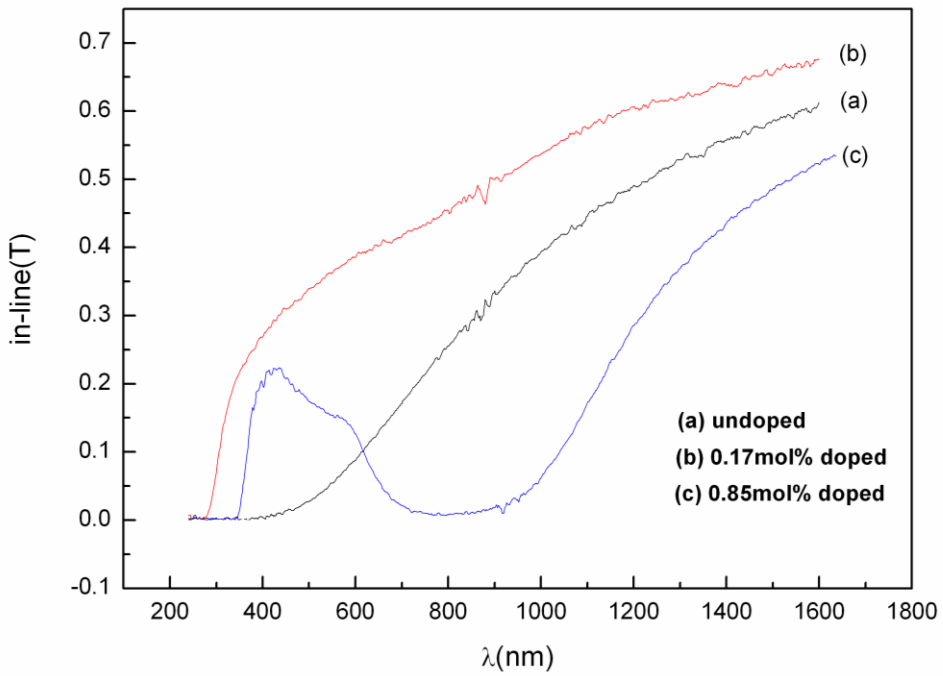

Fig.4-3 In-line transmission result of Ti doped $MgAl_2O_4$ at 1250℃-20min

Namely, the sintering temperature at 1250^{o}C is a little bit low for densification in case for pure $MgAl_2O_4$ although densification can be achieved with addition of Ti at optimum level. In contrast, Ti additives hinders densification at 1300^{o}C in pure $MgAl_2O_4$. Likewise with fig.4-1 which shows transmittance drop in red region, the same tendency is observed by Ti doped $MgAl_2O_4$ at 1250^{o}C. Transmittance is hard to confirm in 1.7mol% Ti doped $MgAl_2O_4$.

In order observe the existence Ti as scattering center, the reflectivity is measured because transmittance is decreased as relatively high Ti concentration. If Ti is added over solubility limit in $MgAl_2O_4$, then Ti cannot be fully form solid solution and it causes scattering. The reflectivity about sintered sample at 1300^{o}C is depicted in Fig.4-5. According to fig.4-5, undoped sample shows the highest reflectivity. This result implies that Ti doping concentration does not affect the reflectivity. And also the reflectivity shows opposite tendency with addition of Ti. This result tells us that the transmittance drop in visible range is related to large absorption in visible light. That is, effect of visible light absorption is bigger than sinterbility improvement due to Ti doping. Therefore, the main factor for transmittance drop can be concluded by visible light absorption.

Fig.4-6 deals with in-line transmission results of over added MgO of non-stoichiometric $MgAl_2O_4$. $MgAl_2O_4$ powder is synthesized by stoichiometric composition of MgO and Al_2O_3, and non-stoichiometric spinel is obtained with increasing ratio of MgO.

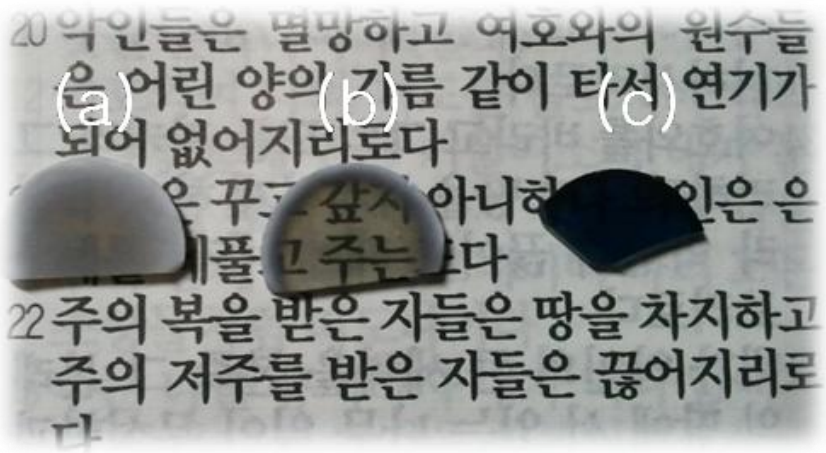

Fig.4-4 The sintered body at 1250℃-20min about x mol% Ti doped $MgAl_2O_4$: (a) undoped, (b) 0.17mol%, (c) 0.85mol%

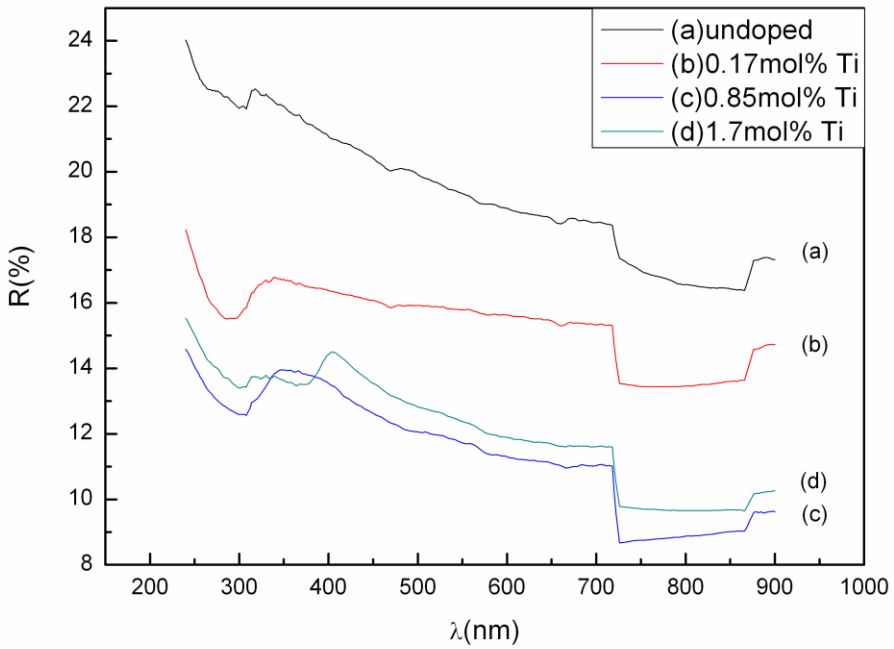

Fig.4-5 Reflectivity result of Ti doped $MgAl_2O_4$ at 1300℃-20min

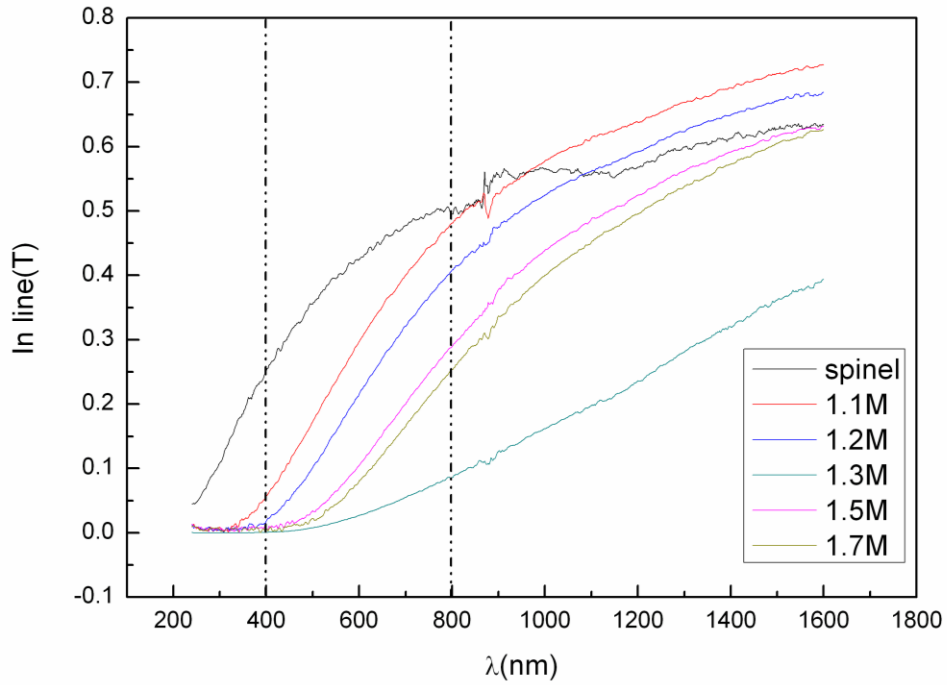

Fig.4-6 MgO rich phase in non-stoichiometric $MgAl_2O_4$($xMgO:Al_2O_3$,x=1.1, 1.2, 1.3 1.5, 1.7)

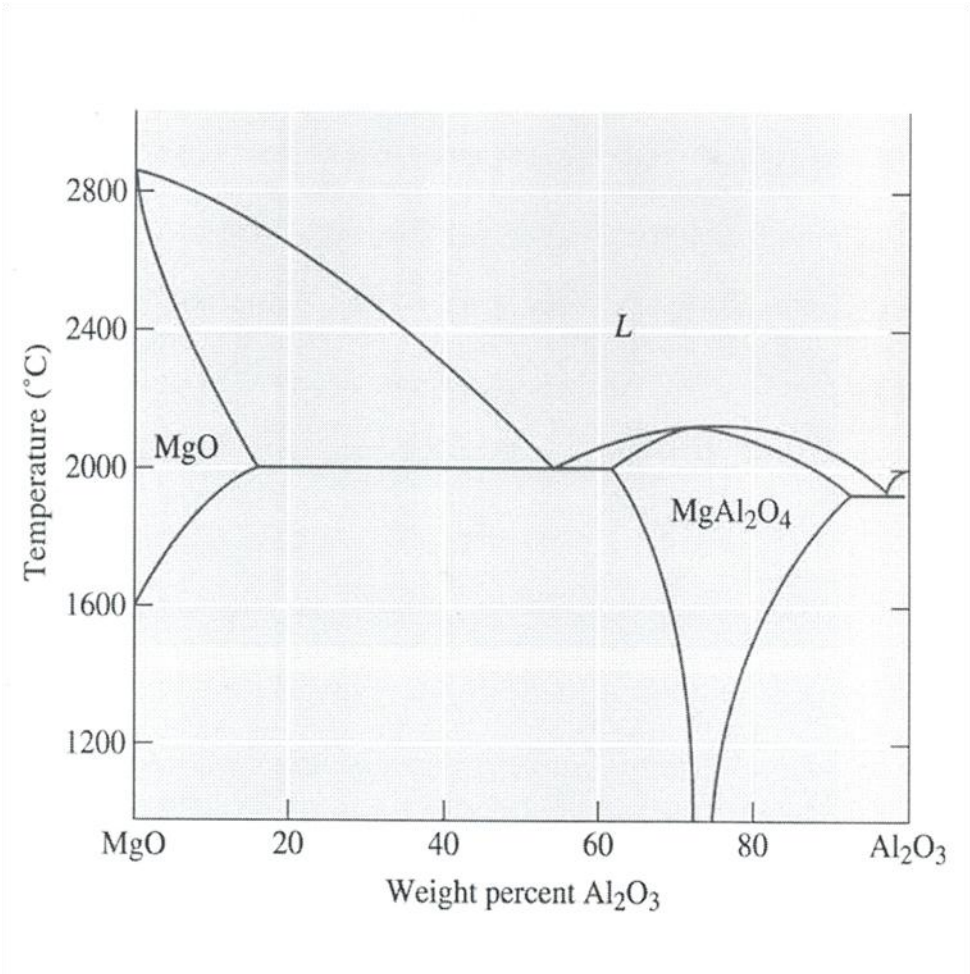

Fig.4-7 $MgAl_2O_4$ spinel phase diagram[63]

The purpose of this experiment is to decline the effect of intrinsic defect as known as MgO deficiency. According to fig.4-6, the transmission of MgO rich phases is rapidly diminished in visible range as increasing MgO contents compare to stoichiometric $MgAl_2O_4$. It seems that MgO phase segregate from $MgAl_2O_4$ due to super saturation. And the segregation of MgO is existed as scattering center. On the other hand, as confirmed in fig.4-7, non-stoichiometric $MgAl_2O_4$ can be maintained in broad range.[63]

Fig.4-8 shows the in-line transmission results derived for over added Al_2O_3 of non-stoichiometric $MgAl_2O_4$. The results of Al_2O_3 rich phase are different from that of MgO rich phase. In case of 1.3 mol% Al_2O_3 additions, the transmission is higher than stoichiometric spinel from 550nm to 800nm in visible range. It suggests that the addition of Al_2O_3 is supported for compensation of intrinsic defect in spinel structure. Also it predicts that the contents of Al_2O_3 as scattering center are lower than MgO because the solubility of Al_2O_3 is higher than MgO through the phase diagram of spinel.

The SEM image of Ti doped $MgAl_2O_4$ at 1300^oC is shown in fig.4-9. From fig.4--9, coarsening of grain is observed with increasing Ti contents. Generally, transmittance decreases by coarsened grain.[53] When the grain size is bigger than the wave length of incident beam, incident lay scatters at grain boundary in transparent ceramics as explained by Snell's law. But $MgAl_2O_4$ has a spinel structure which has symmetrically isotropic, a structure which does not affect to grain boundary scattering by birefringence.[64]

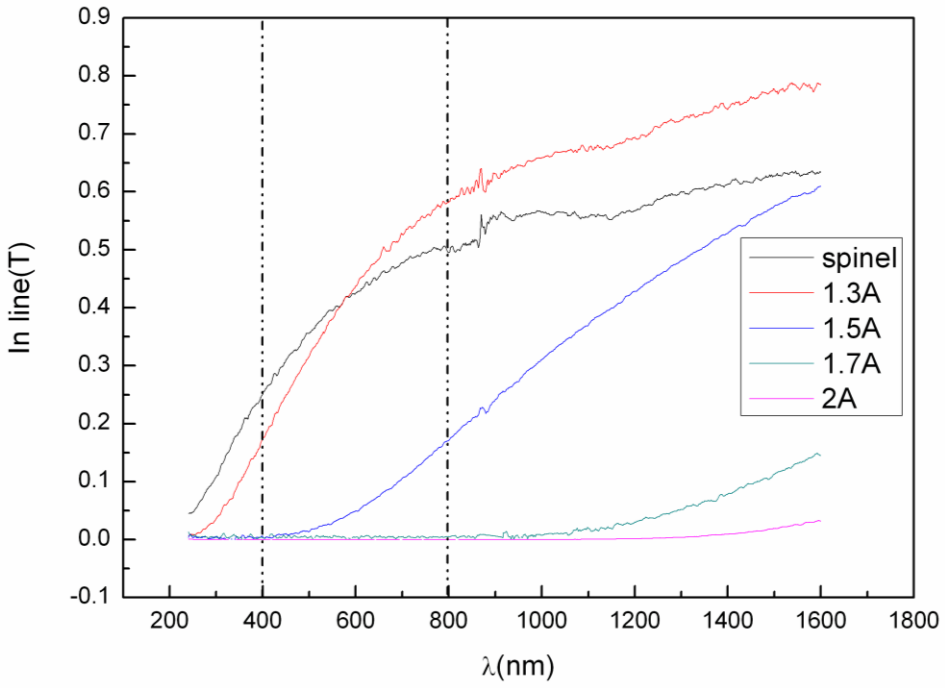

Fig.4-8 Al_2O_3 rich phase in non-stoichiometric $MgAl_2O_4$($MgO:xAl_2O_3$,x=1.3 1.5, 1.7, 2)

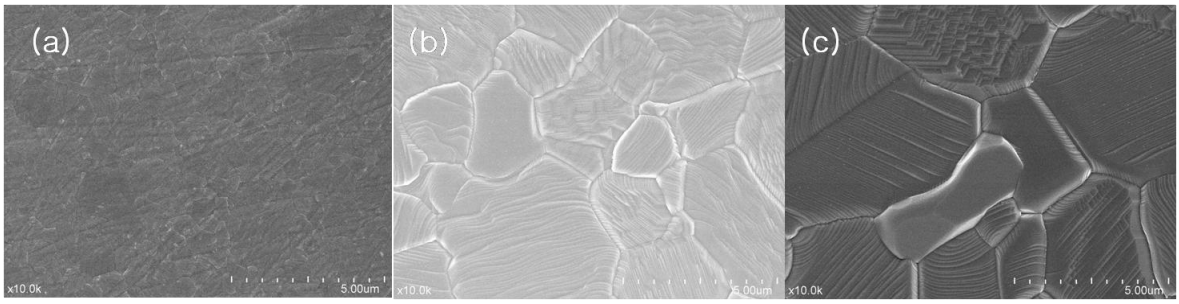

Fig.4-9 The SEM image about Ti doped $MgAl_2O_4$: (a) 0.17mol% Ti, (b) 0.85mol% Ti, (c) 1.7mol% Ti

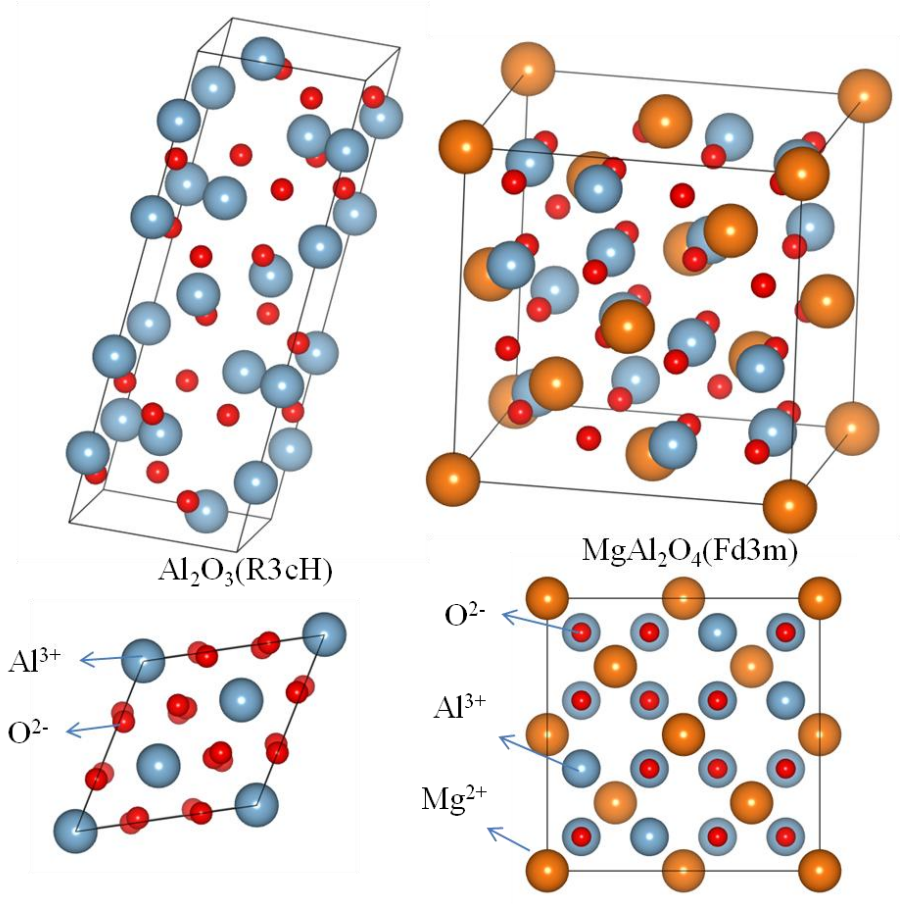

Fig.4-10 The crystal structure about Al_2O_3 and $MgAl_2O_4$

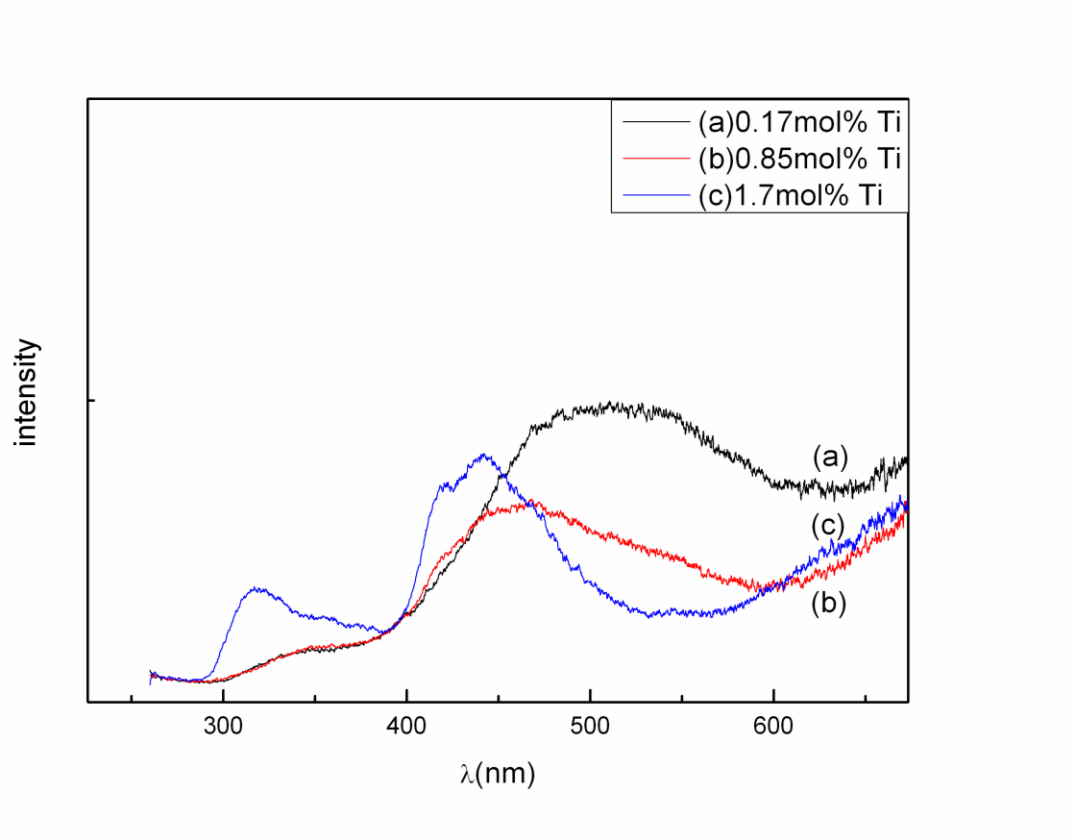

Fig.4-11 The emission results of Ti doped spinel(excitation: 250nm)

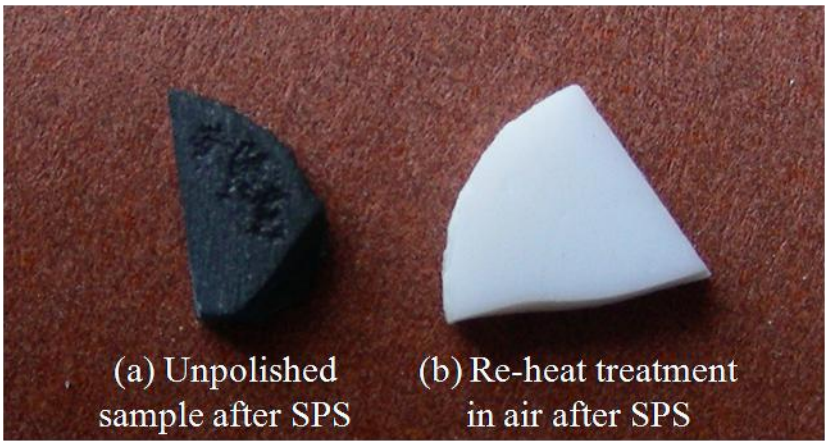

Fig.4-12 the sample images: (a) no heat-treatment after sintering, (b) Re-heat treatment at 1000℃-2h in air after sintering

Detailed reason has not reported yet. So, it is not clear. On the other hands, the grain boundary scattering is detected in case of Al_2O_3 due to its corundum structure.[65]

Fig.4-11 depicts photo luminescence results of sintered sample. Emission peak at 250nm excitation is shifted to shorter wavelength range with addition of Ti. PL results are corresponded to transmittance results which drop in visible range of red color. Also our previous results show that white emission occurs by synthesized powder in air but greenish blue emission appears by that in vacuum.[62] Emission color is determined by a condition of final heat treatment. Most of Ti ions exist as Ti^{3+} in heating condition at vacuum which explains the observation of greenish blue emission. Emission property of poly crystalline Ti doped $MgAl_2O_4$ is well matched with single crystal growth case. Ti addition is well known for compensation of intrinsic defect of Mg^{2+} deficiency, related to red emission, which is eliminated by Ti doping and it contributes to blue shift of emission.

Fig.4-12 is a photograph for 0.85mol% Ti doped sintered body(a: after sintering by SPS, b: re-heat treatment in air after spark plasma sintering). Apparent color of 0.85mol% Ti doped $MgAl_2O_4$ is blue. It has same tendency compare to single crystal(1mol% Ti doped spinel), which turned transparent body after annealing in air.[9] However, colored body changed into white body(fig.4-12b) after annealing in air in case of our poly crystalline spinel.

This result is correlated to improvement of red emission. Lots of Ti^{3+} ions are converted to Ti^{4+} in oxidation atmosphere and excess Mg^{2+} vacancies are generated

by the number of Ti in tetrahedral site due to charge compensation. It is also reported that Mg^{2+} vacancy is contributed to red emission in $MgAl_2O_4$ as intrinsic defect.[9] Also it seems that Shottky pair is formed because Mg^{2+} vacancy combines with O^{2-} vacancy which is located in nearest neighbor. Our previous first principle calculation supported to increase red emission by Schottky pair.[61]

4.4 Conclusion

Ti doped poly crystalline $MgAl_2O_4$ obtained good transmittance and good emission properties by spark plasma sintering in vacuum. This poly crystalline $MgAl_2O_4$, those which has both of properties, has not been reported yet. So, it has many advantages like synthesis method compare to single crystal growth. Transmittance normally decreases with addition of Ti in $MgAl_2O_4$, but 0.17mol% Ti doped sample sintered at 1250^oC is better than undoped $MgAl_2O_4$. This is because addition of Ti can improve not only sinterbility but also absorption in visible range. In spite of these characteristics, the improvement of transmittance can be achieved by sintering under 1300^oC due to sinterbility factor regardless of emission property. Ti doped poly-$MgAl_2O_4$ by prepared under vacuum obtains greenish blue emission at 250nm excitation by charge transfer. Most of Ti ions are left to Ti^{3+} in reduction condition and it corresponds to previous results. As increasing Ti contents, emission seems to be shifting into blue and this emission tendency is considered due to diminishing of red emission from Mg^{2+} deficiency.

In contrast, white emission shows up with compensation of red emission. Remained Ti^{3+} is mostly converted to Ti^{4+} in air during heat treatment and Mg^{2+} deficiency is increased by Ti^{4+} in tetrahedral site. As a result, white emission can be detected because red emission is encouraged by Schottky pair and intrinsic defect.

After annealing, the decline of transmittance at surface can be explained by following reason. Ti atoms, which are located in Mg and Al site, are hard to move

each other site. But Ti^{3+} in Mg site can be oxidized to Ti^{4+} in oxidizing condition. As a result, the transmittance is decayed because Mg^{2+} vacancy is increased and absorption occurs at Mg^{2+} deficiency. According to other literature, when transition metal was doped in Mg site, transmittance was decreased by absorption at visible range.[11] It can predict that Ti is occupied in Mg site because same phenomenon was observed from our result. Also, it implies that lots of Ti^{3+} can be existed after Ti doped $MgAl_2O_4$ was sintered in reduction condition. Therefore, it can be predicted that the transmittance is decreased in sintered body after annealing.

Therefore, $MgAl_2O_4$ research can contribute to industry field for display devices by optimization of sintering condition and Ti contents.

5. Summary and Conclusion

$MgAl_2O_4$, as a wide band gap material, is well known for an outstanding optical, mechanical property and chemical stability. Especially, its optical properties attract attention to many research fields. In this study, we focus on luminescence and transmittance among optical properties. The rare earth has been used to obtain excellent luminescence property in phosphor as a dopant. However, the research is ongoing in order to avoid the use of rare earth. Following this consideration in our study, Ti in transition metal was selected as a dopant in $MgAl_2O_4$.

Firstly, the synthesized powder, which obtained the white emission at 250nm excitation, was prepared by solid state reaction by mixing commercial $MgAl_2O_4$ and TiO_2 in ethanol. The white emission peak is composed of 4 peaks as 440, 490, 550 and 620nm from PL result. Also the coexistence of Ti^{3+} and Ti^{4+} was confirmed by XPS and Rietveld method. It expects that both of Ti ions can be located in tetrahedral and octahedral site. From DV-Xα calculation, the most of the cases are excited by charge transfer between Ti3d and O2p. On the other hand, an electron in $^2T_2$ state can be more easily excited over LUMO level in case of Ti^{3+} in tetrahedral site compare to CT between Ti3d and O2p. Relatively weak emission occurs at 430 and 490nm, while strong emission appeared at 550nm due to Ti^{3+}. According to literature survey, 430nm emission has been explained by only carbon contamination. Aspect of this fact, our research shows a difference. Meanwhile, strong emission at 490 and 620nm is confirmed including weak 550nm emission by Ti^{4+}. 490nm

emission is well matched with other researches. But Mg^{2+} vacancy is generated by the increase in Ti^{4+} in Mg site. Hence, it implies that the red emission is increased by Schottky pair.

Secondly, nano sized Ti doped $MgAl_2O_4$ is prepared by combustion method. In case of nano sized Ti doped $MgAl_2O_4$, bluish white emission is obtained at 250nm excitation. Such as bulk system, the emission peak consisted of 4 different peaks but the emission spectrum is totally shifted to lower wavelength. The reason seems that Ti^{3+} contents is increased in the ratio between Ti^{3+} and Ti^{4+} as dopant in $MgAl_2O_4$ compare to bulk system. Both of the facts are well supported to that hypothesis. Emission phenomenon at 620nm by Schottky pair appeared in bulk system diminishing in nano system can be observed, as well as emission at 720nm is known to removed by Ti^{4+} in octahedral site is still remaining. Meanwhile, the emission spectrum of Ti doped nano $MgAl_2O_4$ is observed at 360nm as well as 250nm. This is not the effect of Ti inside $MgAl_2O_4$ but Ti on surface is contributing the emission at 360nm excitation in Ti doped nano $MgAl_2O_4$. This fact can be considered in nano system which easily supplies doping site on surface and normally generates defects on surface. Also Ti is detected in Mg site by HR-STEM. Therefore, this evidence can be supported to our theory.

Lastly, Ti doped poly crystalline $MgAl_2O_4$ obtained good transmittance and good emission properties by spark plasma sintering in vacuum. This poly crystalline $MgAl_2O_4$, those which has both of properties, has not been reported yet. So, it has many advantages like synthesis method compare to single crystal growth.

Transmittance normally decreases as Ti added in $MgAl_2O_4$ but 0.17mol% Ti doped sample sintered at 1250^oC is better than undoped $MgAl_2O_4$. Because addition of Ti can improve not only sinterbility but also absorption in visible range. Ti doped poly-$MgAl_2O_4$ by prepared under vacuum obtains greenish blue emission at 250nm excitation by charge transfer. Most of Ti ions are left to Ti^{3+} in reduction condition and it corresponds to previous results. As increasing Ti contents, emission seems to be shifting into blue and emission tendency is considered due to diminishing of red emission from Mg^{2+} deficiency.

In conclusion, the emission color can be tuned by synthesis method and condition in Ti doped $MgAl_2O_4$ because the luminescence property of phosphor is determined by doping site and the charge valence of dopant. If the optimized condition for synthesis is fixed through further work, then the properties can be improved. And it can be fabricated for industry field.

6. Further work to be done

<Part.3>

1. In order to confirm the size of powder, TEM image has to be measured for synthesized powder at 1000^{o}C.
2. Although nano powder was synthesized in oxidation condition, Ti^{3+} dominantly existed in nano Ti doped $MgAl_2O_4$. But we cannot explain why Ti^{3+} is mostly remained after synthesis. So, further work has to be proceeded for example, thermodynamic study.
3. The white emission at 360nm excitation was explained by Ti^{4+} on the surface of nano Ti doped $MgAl_2O_4$ because emission property was decided by the charge valence of dopants and doping site. However, Ti^{3+} and Ti^{4+} in both of sites(Mg and Al) was already proved through emission at 250nm excitation. Moreover, different luminescence properties were reported in nano materials by dopants on surface. So, we want to confirm Ti^{4+} on the surface by XPS. But reliable data cannot be derived due to relatively weak intensity. We expect that strong intensity can be observed by XPS if the synthesized powder can be spoiled on carbon tape. Then Ti^{4+} on the surface can be distinguished from binding energy shift.

<Part.4>

1. Transmittance of sintered body was removed by annealing at oxidation

atmosphere. In order to obtain transparent body by Reversible process after annealing, additional experiments have to be done using vacuum furnace.

7. References

1. Yanfang, Z., Lan, L., Xiaosong, Z. & Qun, X. , *J. Rare Earth*, **26**, 446–449 (2008)
2. Xianquing, P., Machida, K-I., Horikawa, T. & Hanzawa, H., *J. Rare Earth*, **26**, 198–202 (2008).
3. Lombard, P., Boizot, B., Ollier, N., Jouini, A. & Yoshikawa, A., *J. Cryst. Growth*, **311**, 899–903 (2009).
4. Zhong, R., Zhang, J., Wei, H., Qi, X., Li, M. & Han, X., *Chem. Phys. Lett.* **508**, 207–209 (2011).
5. Hassanzadeh-Tabrizi, S. A., *Opt. Mater.* **33**, 1607–1609 (2011)
6. Irifune, T., Fujino, K. & Ohtani, E., *Nature*, **349**, 409–411 (1991).
7. Omkaram, I., Vengala Rao, B. & Buddhudu, S., *J. Alloy. Compd*. **474**, 565–568 (2009).
8. Fujimoto, Y., Tanno, H., Izumi, K., Yoshida, S., Miyazaki, S., Shirai, M., Tanaka, K., Kawabe, Y. & Hanamura, E., *J. Lumin.* **128**, 282–286 (2008).
9. Sato, T., Shirai, M., Tanaka, K., Kawabe, Y. & Hanamura, E., *J. lumin.* **114**, 155–161 (2005).
10. Jouini, A., Yoshikawa, A., Brenier, A., Fukuda, T. & Boulon, G., *Phys. Status Solidi C* **4**, 1380–1383 (2007)
11. Izumi, K., Miyazaki, S., Yoshida, S., Mizokawa, T. & Hanamura, E.,

Phys. Rev. B **76**, 075111 (2007)

12. Peng, L., Wang, Y., Wang, Z. & Dong, Q., *Appl. Phys. A-Mater*. 102, 387–392 (2011).

13. Wu, Z-C., Liu, J., Hou, W-G., Xu, J. & Gong, M-L., *J. Alloy. Compd*. **498**, 139–142 (2010).

14. Sivakumar, V., & Varadaraju, U. V., *J. Electrochem. Soc.* **156**, J179–J184 (2009).

15. Jiao, H., & Wang, Y., *J. Electrochem. Soc.* **156**, J117–J120 (2009).

16. Kim, Y., & Kang, S., *Acta Mater.* **59**, 3024–3031(2011).

17. Adachi, H., Tsukada, M., & Satoko, C., *J. Phys. Soc. Jpn.* **45**, 875–883 (1978).

18. Slater, J. C., *Phys. Rev.* **81**, 385 (1951).

19. Kim, Y., & Kang, S., *Acta Mater.* **59**, 126–132 (2011).

20. Henderson, C. M. B., Charnock, J.M., & Plant, D.A., *J. Phys. Condens. Mat.* **19**, 076214 (2007).

21. Poe, B. T., McMillan, P. F., Cotė, B., Massiot, D. & Coutures, J. P., *Science*, **259**, 786–788 (1993).

22. Meng, X., & Tanaka, K., *Appl. Phys. Lett.* **90**, 051917 (2007).

23. Page, P. S., Dhabekar, B. S., Bhatt, B. C., Dhoble, A. R. & Godbole, S. V., *J. Lumin.* **130**, 882–887 (2010).

24. Emeline, A. V., Kataeva, G. V., Ryabchuk V. K. & Serpone, N., *J. Phys. Chem.* B **103**, 9190–9199 (1999).

25. Blasse, G., & Grabmaier, B. C. Luminescent Materials., p. 20, Springer-Verlag (1994).

26. Ball, J. A., Murphy, S. T., Grimes, R. W., Bacorisen, D., Smith, R., Uberuaga, B. P. & Sickafus, K. E., *Solid state Sci.* **10**, 717–724 (2008).

27. Cui, S., Jiao, H., Li, G. & Su, M., *J. Electrochem. Soc.* **157**, J88–J91 (2010).

28. P. S. Chowdhury, P. Sen, A. Patra, "Optical properties of CdS nanoparticles and the energy transfer from CdS nanoparticles to Rhodamine 6G", Chem. Phys. Lett, 413, 311-314, 2005

29. P. R. Fragoso, G. G. de la Cruz, S. A. Tomas, J. G. M. Alvarez, O. Z. Angel, "Photoluminescence of CdS nanoparticles embedded in a starch matrix", J. of Lumin., 130, 1128-1133, 2010

30. C. Borriello, S. Masala, V. Bizzarro, G. Nenna, M. Re, E. Pesce, C. Minarini, T. D. Luccio, "Electroluminescence properties of poly(3-hexylthiophene)-Cadmium Sulfide nanoparticles grown in situ", J. of Appl. Poly. Sci., 122, 3624-3629, 2011

31. S. Ithurria, M. D. Tessier, B. Mahler, R. P. S. M. Lobo, B. Dubertret, A. L. Efros, "Colloidal nanoplatelets with two dimensional electronic

structure", Nature Materials, 10, 936-941, 2011

32. M. T. Frederisk, V. A. Amin, L. C. Cass, E. A. Weiss, "A molecule to detect and perturb the confinement of charge carriers in Quantum dots", Nano Lett., 11, 5455-5460, 2011

33. S. Ithurria, B. Dubertret, "Quasi 2D colloidal CdSe platelets with thicknesses controlled at the atomic level", J. of Am. Chem. Soc., 130, 16504-16505, 2008

34. M. W. Blair, L. G. Jacobsohn, B. L. Bennett, R. E. Muenchausen, S. C. Sitarz, J. F. Smith, D. W. Cooke, P. A. Crozier, R. Wang, "Structure and luminescence of Ce doped Lu_2SiO_5 nanophosphor", Mater. Res. Soc. Symp. Proc., 1056, 1-6, 2008

35. F. Gu, C. Z. Li, H. B. Jiang, "Combustion synthesis and photoluminescence of MgO:Eu^{3+} nanocrystals with Li^+ addition", J. of Cry. Crowth., 289, 400-404, 2006

36. J. Zheng, P. R. Nicovich, R. M. Dickson, "Highly fluorescent noble metal Quantum dots", Annu. Rev. Phys. Chem., 58, 409-431, 2007

37. M. A. H. Muhammed, S. Ramesh, S. S. Sinha, S. K. Pal, T. Pradeep, "Two distinct fluorescent Quantum clusters of gold starting from metallic nanoparticles by pH-dependent ligand etching", Nano Res., 1, 333-340, 2008

38. R. Philip, P. Chantharasupawong, H. Qian, R. Jin, J. Thomas, "Evolution of nonlinear optical properties: From gold atomic clusters to plasmonic

nanocrystals", Nano Lett., dx.doi.org/10.1021/nl301988v, 2012

39. A. Moores, F. Goettmann, "The Plasmon band in noble metal nanoparticles: an introduction to theory and applications", New J. Chem., 30, 1121-1132, 2006
40. S. Stankic, M. Sterrer, P. Hofmann, J. Bernardi, O. Diwald, E. Knozinger, "Novel optical surface properties of Ca^{2+} doped MgO nanocrystals", Nano Lett., 5, 1889-1893, 2005
41. S. A. H. Tabrizi, "Polymer assisted synthesis and luminescence properties of $MgAl_2O_4$:Tb nanopowder", Optical Materials, 33, 1607-1609, 2011
42. X. Y. Chen, C. Ma, S. P. Bao, "$MgAl_2O_4:Eu^{3+}$ nanoplates and nanoparticles as red emitting phosphors: Shape controlled synthesis and photoluminnescent properties", Solid State Science, 12, 857-863, 2010
43. J. Lee, J. Bang, H. Yang, "Highly stable colloidal ZnO nanocrystals by MgO passivation", J. Phys. D:Appl. Phys., 42, 1-6, 2009
44. N. Y. Gross, M. S. Harari, M. Zimin, S. Kababya, A. Schmidt, N. Tessler, "Molecular control of quantum-dot internal electric field and its application to CdSe-based solar cells", Nature Materials, 10, 974-979, 2011
45. P.S. Sokolov, A. N. Baranov, V. A. Tafeenko, V. L. Solozhenko, "High pressure synthesis of $LiMeO_2$-ZnO($Me=Fe^{3+}$, Ti^{3+}) solid solutions with a rock salt structure", High Pressure Research, 31, 304-309, 2011
46. M. A. A. Issa, N. M. Molokhia, Z. H. Dughaish, "Effect of cerium oxide(CeO_2) additives on the dielectric properties of $BaTiO_3$ ceramics", J. Phys. D: Appl. Phys., 16, 1109-1114, 1983

47. C. Singh, S. B. Narang, I. S. Hudiara, Y. Bai, K. Marina, “Hysteresis analysis of Co-Ti substituted M-type Ba-Sr hexagonal ferrite”, Materials Letters, 63, 1921-1924, 2009

48. T.-L. Phan, S.-C. Yu, M.-H. Phan, T. P. J. Han, “Photoluminescence properties of Cr^{3+}-doped $MgAl_2O_4$ natural spinel”, J. of Kor. Phys. Soc., 45, 63-66, 2004

49. Y. Liu, J. Liu, C. C. Liu, R. L. Niu, L. H. Zheng, L. B. Su, J. Xu, “Pulse Chracteristics of passively Q-switched 1.34μm Nd:$GdVO_4$/Co^{2+}:$MgAl_2O_4$ Laser”, Solid state and liquid lasers, 21, 472-476, 2011

50. V. Singh, MD. M. Haque, D.-K. Kim, “Investigation of a new red-emitting, Eu^{3+}-activated $MgAl_2O_4$ phosphor”, Bull. Kor. Chem. Soc., 28, 2477-2480, 2007

51. B.N. Kim, K. Hiraga, K. Morita, H. Yoshida, “Effect of heating rate on microstructure and transparency of spark plasma sintered alumina”, J. of Eur. Ceram. Soc., 29, 323-327, 2009

52. B.N. Kim K. Morita, J. Lim, K. Hiraga and H. Yoshida, “Effects of preheating of powder before spark plasma sintering of transparent $MgAl_2O_4$ spinel”, J. of Am. Cer. Soc., 93(8), 2158-2160, 2010

53. R. Apetz and Michel P.B. van Bruggen, “Transparent Alumina: A Light

scattering model", J. of Am. Cer. Soc., 86(3), 480-486, 2003

54. B.N. Kim, K. Hiraga, K. Morota, H. Yoshida, Y. Kagawa, "Light scattering in MgO-doped alumina fabricated by spark plasma sintering", Acta. Met., 58, 4527-4535, 2010

55. D.-S. Kim, J.-H. Lee, R. J. Sung, S. W. Kim, H. S. Kim, J. S. Park, "Improvement of translucency in Al_2O_3 ceramics by two-step sintering technique", J. of Eur. Cer. Soc., 27, 3629-3632, 2007

56. R. Chaim, R. Marder, C. Estournes, "Optically transparent ceramics by spark plasma sintering of oxide nanoparticles", Scripta Materialia, 63, 211-214, 2010

57. B.-N. Kim, K. Hiraga, K. Morita, H. Yoshida, "Spark plasma sintering of transparent alumina", Scripta Materialia, 57, 607-610, 2007

58. C. Wang, Z. Zhao, "Transparent $MgAl_2O_4$ ceramic produced by spark plasma sintering", Scripta Materialia, 61, 193-196, 2009

59. H. B. Zhang, B.-N. Kim, K. Morita, H. Yoshida, J. Lim, K. Hiraga, "Optimization of high-pressure sintering of transparent zirconia with nano-sized grains", J. of alloys and compounds, 508, 196-199, 2010

60. H. Zhang, B.-N. Kim, K. Morita, H. Yoshida, J. Lim, K. Hiraga, "Optical properties and microstructure of nanocrystalline cubic zirconia prepared by high-pressure spark plasma sintering", J. of Am. Ceram. Soc., 94,

2981-2986, 2011

61. J. Lim, B.N. Kim, Y. Kim, S. Kang, R.J. Xie, I.S. Chong, K. Morita, K. Hiraga, “White emission: $MgAl_2O_4$”

62. A. Jouini, H. Sato, A. Yoshikawa, T. Fukuda, G. Boulon, K. Kato, E. Hanamura, “Crystal growth and optical absorption of pure and Ti, Mn-doped $MgAl_2O_4$ spinel”, J. of Crystal Growth, 287, 313-317, 2006

63. D. Kim, “Effect of additive on the sintering of stoichiometric $MgAl_2O_4$-spinel”, thesis in Seoul Nat’l Univ., 2009

64. K. Morita, B.N. Kim, K. Hiraga, and H. Yoshida, “Fabrication of transparent $MgAl_2O_4$ spinel polycrystal by spark plasma sintering processing”, Scripta Materialia, 58, 1114-1117, 2008

65. M. Stuer, Z. Zhao, U. Aschauer, P. Bowen, “Transparent polycrystalline alumina using spark plasma sintering: Effect of Mg, Y and La doping”, J. of Eur. Ceram. Soc., 30, 1335-1343, 2010

초 록

$MgAl_2O_4$ spinel은 흥미로운 전기적, 기계적, 자성적, 광학적 특성 때문에 여러 분야의 적용을 위해 연구되어 왔다. 더욱이 $MgAl_2O_4$ spinel은 광 소자를 위한 모체로도 널리 알려져 있다. 본 연구에서는 티타늄을 $MgAl_2O_4$ 모체에 도핑하여 단결정 성장으로부터 얻은 청색 발광과는 달리 티타늄 도핑으로부터 백색 발광을 얻었다. 또한 이런 발광 특성을 제 1원리를 이용한 DV-Xα 로부터 얻은 에너지 다이어그램을 이용하여 설명하였다. 백색 발광 피크는 250㎚ 여기광에서 440, 490, 550, 620㎚의 4개 피크로 구성된다. 한편, Ti^{3+}가 4배위 자리에 있을 경우와 Ti^{4+}가 8배위의 자리를 점유하고 있을 때, 490㎚와 550㎚에 해당하는 녹청색 발광에 기여함을 밝혔다. 반면에 적색 발광에 해당하는 620~710㎚ 영역대의 발광은 Mg^{2+}와 O^{2-} 공공에 의해서 발생하였다.

또한 combustion method를 이용하여 티타늄이 도핑된 나노 $MgAl_2O_4$를 합성에 성공 하였다. 벌크 형광체와 마찬가지로 백색 발광을 보였으나 상대적으로 Ti^{3+}의 비가 많아져 청색의 발광을 포

함하였다. 나노 $MgAl_2O_4$에서의 발광 피크도 벌크와 마찬가지로 동일한 4개의 피크로 구성되었다. 이는 250㎚ 여기광에서 벌크의 발광 현상과 동일한 현상에 의해 발광이 되는 것으로 나타났다. 반면에 360㎚ 여기광에서도 청백색 발광을 보였는데 이는 나노 $MgAl_2O_4$ 표면에 위치한 티타늄이 발광 소스로 작용하였음을 밝혔다.

한편, 통전 가압 소결을 통하여 티타늄이 도핑된 $MgAl_2O_4$ 소결체를 얻을 경우 좋은 투과 특성과 함께 청색 발광을 보였다. 소결시 진공분위기에서 열처리가 진행됨으로 인하여 청색 발광을 보였다. 이는 백색 발광과는 달리 환원 분위기에 의해 Ti^{3+}가 주로 존재하기 때문이다. 희토류 족 원소의 첨가없이 백색 발광 및 청색 발광의 구현이 가능한 티타늄이 도핑된 $MgAl_2O_4$는 앞으로 많은 연구가 주목된다.

핵심어: $MgAl_2O_4$, phosphor, rare earth, nano, transparent, white emission

학 번: 2005-20947